



IMMUNOPATHOLOGY AND INFECTIOUS DISEASES

# The Thyroid Hormone Triiodothyronine Controls Macrophage Maturation and Functions

## Protective Role during Inflammation

Cristiana Perrotta,<sup>\*</sup> Marcella Buldorini,<sup>†</sup> Emma Assi,<sup>\*</sup> Denise Cazzato,<sup>†</sup> Clara De Palma,<sup>\*</sup> Emilio Clementi,<sup>\*†</sup> and Davide Cervia<sup>\*‡</sup>

From the Unit of Clinical Pharmacology,<sup>\*</sup> Department of Biomedical and Clinical Sciences, National Research Council Institute of Neuroscience, Luigi Sacco University Hospital, University of Milan, Milan; the E. Medea Scientific Institute,<sup>†</sup> Bosisio Parini; and the Department for Innovation in Biological, Agro-Food and Forest Systems,<sup>‡</sup> University of Tuscia, Viterbo, Italy

Accepted for publication  
October 4, 2013.

Address correspondence to  
Davide Cervia, Ph.D., Department for Innovation in Biological, Agro-Food and Forest Systems, Università della Tuscia, Largo dell'Università snc, Viterbo 01100, Italy; or Emilio Clementi, Ph.D., Department of Biomedical and Clinical Sciences, Luigi Sacco University Hospital, Università di Milano, via GB Grassi 74, Milano 20157, Italy. E-mail: [d.cervia@unitus.it](mailto:d.cervia@unitus.it) or [emilio.clementi@unimi.it](mailto:emilio.clementi@unimi.it).

The endocrine system participates in regulating macrophage maturation, although little is known about the modulating role of the thyroid hormones. *In vitro* results demonstrate a negative role of one such hormone, triiodothyronine ( $T_3$ ), in triggering the differentiation of bone marrow-derived monocytes into unpolarized macrophages.  $T_3$ -induced macrophages displayed a classically activated (M1) signature. A  $T_3$ -induced M1-priming effect was also observed on polarized macrophages because  $T_3$  reverses alternatively activated (M2) activation, whereas it enhances that of M1 cells. *In vivo*, circulating  $T_3$  increased the content of the resident macrophages in the peritoneal cavity, whereas it reduced the content of the recruited monocyte-derived cells. Of interest,  $T_3$  significantly protected mice against endotoxemia induced by lipopolysaccharide i.p. injection; in these damaged animals, decreased  $T_3$  levels increased the recruited (potentially damaging) cells, whereas restoring  $T_3$  levels decreased recruited and increased resident (potentially beneficial) cells. These data suggest that the anti-inflammatory effect of  $T_3$  is coupled to the modulation of peritoneal macrophage content, in a context not fully explained by the M1/M2 framework. Thyroid hormone receptor expression analysis and the use of different thyroid hormone receptor antagonists suggest thyroid hormone receptor  $\beta_1$  as the major player mediating  $T_3$  effects on macrophages. The novel homeostatic link between thyroid hormones and the pathophysiological role of macrophages opens new perspectives on the interactions between the endocrine and immune systems. (*Am J Pathol* 2014, 184: 230–247; <http://dx.doi.org/10.1016/j.ajpath.2013.10.006>)

Accumulating evidence indicates that the endocrine and immune systems engage in a complex cross talk. Hormones and endocrine transmitters bind to immune system cells, leading to production of factors that modify immune cell functions and tune immune responses.<sup>1</sup> Several studies have addressed the role of different hormones, including growth hormone, leptin, insulin-like growth factor-1, steroid hormones, thyroid-stimulating hormone, prolactin, and neurohypophyseal hormones, in the immune system.<sup>1–5</sup> Comparatively, our understanding of the role, as immunomodulating factors, of the thyroid hormones (THs) 3,3',5'-triiodo-L-thyronine ( $T_3$ ) and L-thyroxine ( $T_4$ ), is still rather incomplete,<sup>6</sup> despite the significant role played by these

molecules in complex function in which the immune system participates, including differentiation, growth, and metabolism.<sup>7,8</sup> Reports focusing mainly on natural killer cells, effector B and T lymphocytes, and dendritic cells revealed that THs may support the basal functions of immune cells, although contradictory results are reported regarding the effect of hypohyperthyroidism on immunity.<sup>6,9–12</sup> In particular, scant information exists about the role of THs in modulating the functions of macrophages, despite the fact

Supported by the Italian Association on Cancer Research grant IG11365 (E.C.) and the Italian Board of Education, University and Research grant PRIN2010-2011 (E.C. and D.C.).

that these monocyte-derived immune-competent cells play key roles in innate and adaptive immunity<sup>13,14</sup> and that THs may change the level of cytokines involved in their function.<sup>6</sup> The magnitude of macrophage inflammatory response is stimulated in rats during the hypothyroid condition and inhibited during the hyperthyroid condition; in addition, in hyperthyroid rats, phagocytic activity and hydrogen peroxide release by macrophages are suppressed.<sup>15</sup> In hypothyroid rats, conversely, macrophage phagocytosis and reactive oxygen species release are both enhanced.<sup>16</sup> T<sub>4</sub> and, in some cases, T<sub>3</sub> were shown to stimulate mouse macrophage phagocytosis.<sup>17–20</sup> THs were also suggested to increase mouse peritoneal macrophage chemotaxis *in vitro*.<sup>21</sup> Recently, a beneficial role of THs in macrophage-mediated meningococcal infection has also been demonstrated.<sup>20</sup>

Macrophages perform an important immune surveillance role through their ability to sense and adapt to local microenvironmental signals.<sup>13</sup> Two distinct states of polarized activation for macrophages have been recognized: the classically activated (M1) macrophage phenotype and the alternatively activated (M2) macrophage phenotype.<sup>13,22,23</sup> The M1 macrophages are activated by Toll-like receptor ligands, such as lipopolysaccharide (LPS) and interferon- $\gamma$  (IFN- $\gamma$ ), express proinflammatory cytokines, mediate defense of the host from a variety of bacteria, protozoa, and viruses, and have roles in antitumor immunity. The M2 macrophages are stimulated by IL-4 or IL-13 and have anti-inflammatory, protumoral function and regulate wound healing.<sup>13,23,24</sup>

The classic genomic actions of THs are mediated by ligand-inducible transcription factors that are members of the steroid/thyroid hormone receptor superfamily. There are two types of TH nuclear receptors (TRs) encoded by TR $\alpha$  and TR $\beta$  genes.<sup>7,25</sup> TR $\alpha$  has one T<sub>3</sub>-binding splice product, TR $\alpha$ 1, and two non-T<sub>3</sub>-binding splice products, TR $\alpha$ 2 and TR $\alpha$ 3, with several additional truncated forms. TR $\beta$  has three major T<sub>3</sub>-binding splice products: TR $\beta$ 1, TR $\beta$ 2, and TR $\beta$ 3. The expression of the mRNAs coding for TR $\alpha$  and TR $\beta$  has been reported in bone marrow-derived macrophages<sup>26</sup>; however, the presence of TR proteins and the effects of TH on macrophage differentiation and M1/M2 macrophage activation are unknown.

In the present study, we have investigated the role of the T<sub>3</sub> system in the regulation of growth/development and functional phenotype of unpolarized macrophages, as well as its influence on M1 or M2 activation. We demonstrate that macrophages, at different stages of growth, express the mRNAs of the two major TR isoforms, TR $\alpha$ 1 and TR $\beta$ 1, but only TR $\beta$ 1 was detected at the protein level. The action of T<sub>3</sub> at intracellular TRs (likely at TR $\beta$ 1) consists of the regulation of unpolarized macrophage, M1, or M2 development. By comparative analysis of euthyroid and hypothyroid animals, we also found that this function by T<sub>3</sub> is reflected in the profile of peritoneal macrophages, indicating the functional relevance of the interactions of TH/macrophages in basal conditions and during systemic inflammation.

## Materials and Methods

### Animals

Experiments were performed on C57BL/6J female mice at 12 to 18 weeks after birth (20 to 30 g body weight). Animals were kept in a regulated environment (23°C  $\pm$  1°C, 50%  $\pm$  5% humidity) with a 12-hour light/dark cycle (lights on at 8 AM). All studies were conducted in accordance with the Italian law on animal care number 116/1992 and the European Communities Council Directive EEC/609/86. The experimental protocols were also approved by the Ethics Committee of the University of Milan (Milan, Italy). All efforts were made to reduce both animal suffering and the number of animals used.

### Isolation of Bone Marrow-Derived Cells, Differentiation, and Activation of Macrophage Primary Cultures

By using published protocols,<sup>27,28</sup> bone marrow precursors from the femur and tibia of mice were isolated and propagated for 8 days in  $\alpha$ -minimum essential medium (37°C, 5% CO<sub>2</sub> in a humidified atmosphere) containing 10% fetal bovine serum (FBS) in the presence of 100 ng/mL macrophage-specific colony-stimulating factor (M-CSF) to generate macrophages (Supplemental Figure S1). Adherent cells were then collected and cultured in the presence of 10 ng/mL M-CSF to form monolayers of differentiated, unpolarized macrophages. Cells were cultured for 2 additional days in the presence of 50 ng/mL IFN- $\gamma$  to generate activated, polarized M1 cells<sup>24</sup> and for 4 additional days with 10 ng/mL IL-4 and 10 ng/mL M-CSF to generate activated, polarized M2a cells.<sup>24</sup> In agreement with previous reports,<sup>28,29</sup> the morphological characteristics of M1 cells appeared flattened and rounded, with different cells displaying a fried egg-like shape, whereas M2 cells were more stretched and elongated (spindle-like morphological features) (Supplemental Figure S2A). Unpolarized macrophage cells appeared adherent, with the characteristic intermediate morphological characteristics of polarized macrophages, with some cells being more elongated, whereas others were more rounded.

### *In Vitro* T<sub>3</sub> Treatments

The thyroid gland produces mainly T<sub>4</sub>, but other tissues deiodinate it to the more potent hormone, T<sub>3</sub>. In our experiments, T<sub>3</sub> or, when indicated, the integrin  $\alpha$ V $\beta$ 3 antagonist, tetraiodothyroacetic acid (tetrac; Sigma-Aldrich, St. Louis, MO), and the TR antagonist, 1-850, were added daily to the medium. Parallel cultures were maintained with T<sub>3</sub> vehicle and used as a control. During treatments, all cells were exposed to 10% TH-depleted FBS-containing medium.<sup>7</sup> Routinely, TH-depleted FBS-containing medium was added 1 to 2 days before T<sub>3</sub> treatment.<sup>30</sup> TH-depleted FBS was obtained by adsorption of FBS onto analytical-grade anion exchange resin (AG 1-X8 Resin, 200 to 400 mesh,

**Table 1** Antibodies and Dilutions Used in Flow Cytometry Analysis, Western Blot Analysis, and Immunofluorescence Microscopy of Macrophages

Primary antibody	Isotype	Dilution	Secondary antibody	Dilution
PE hamster polyclonal anti-CD11c: 117308	IgG	1:100 (FC)	—	—
APC rat monoclonal anti-CD14: 560634	IgG1	1:100 (FC)	—	—
APC hamster polyclonal anti-CD34: 128612	IgG	1:100 (FC)	—	—
FITC rat monoclonal anti-CD68: SM1550FS	IgG2a	1:250 (FC)	—	—
PE rat polyclonal anti-CD206: 141706	IgG2a	1:100 (FC)	—	—
FITC rat monoclonal anti-F4/80: BM4008FS	IgG2b	1:500 (FC), 1:50 (IF)	—	—
Rabbit polyclonal anti-TR $\alpha$ / $\beta$ : sc-772	IgG	1:500 (WB)	HRP—anti-rabbit	1:2000
Goat polyclonal anti-TR $\alpha$ 1: sc-10819	IgG	1:50 (IF)	Alexa Fluor 546 anti-goat	1:500
Rabbit polyclonal anti-TR $\beta$ : ab53170	IgG	1:500 (WB)	HRP—anti-rabbit	1:2000
Mouse monoclonal anti-TR $\beta$ 1: sc-738	IgG	1:50 (IF, FC)	Alexa Fluor 546 anti-mouse	1:500
Rabbit polyclonal anti-arginase 1: sc-20150	IgG	1:5000 (WB)	AP—anti-rabbit	1:10,000
Mouse monoclonal anti- $\beta$ -actin: A5441	IgG1	1:10,000 (WB)	HRP—anti-mouse	1:5000

AP, alkaline phosphatase; APC, allophycocyanin; FC, flow cytometry; FITC, fluorescein isothiocyanate; HRP, horseradish peroxidase; IF, immunofluorescence; PE, phycoerythrin; WB, Western blot analysis.

chloride form), according to the manufacturer-recommended procedure (Bio-Rad, Hercules, CA).

### Immunophenotyping by Flow Cytometry

To determine the expression of several cell surface markers on macrophages, a fluorescence-activated cell sorter analysis was performed. In brief, collected cells were washed with PBS supplemented with 2% FBS and incubated with different antibodies for 1 hour at 4°C. After washing, the extent of marker expression in duplicate samples was analyzed using an FC500 Dual Laser system (Beckman Coulter, Brea, CA). Unstained, single stains, and fluorescence minus one controls were used for setting compensation and gates. Irrelevant isotypic monoclonal antibodies were routinely used as negative controls. FCS Express, version 3 (De Novo System, Portland, OR), was then used for data analysis. When indicated, mean fluorescence intensity (MFI; arbitrary units) was determined as a measure of the extent of marker cell surface expression, excluding cells negative to the staining.

As listed in Table 1, the cell markers used were F4/80, a member of the epidermal growth factor—transmembrane 7 family, CD68 (macrosialin), a member of the lysosomal-associated membrane protein family with a macrophage-specific mucin-like extracellular domain, the integrin  $\alpha$  X chain protein CD11c (CR4), CD14, a glycosylphosphatidyl inositol—linked membrane glycoprotein, the mannose receptor 1 CD206, and CD34, a member of a family of single-pass transmembrane proteins. F4/80, CD68 (conventional pan-macrophage markers),<sup>13,31,32</sup> and CD11c (conventional dendritic cell marker) are commonly used to distinguish macrophages from dendritic cells.<sup>13,33,34</sup> CD14 and CD206 are highly expressed in M1 or M2a cells, respectively,<sup>24</sup> whereas CD34 shows distinct expression on early hematopoietic precursors and vascular-associated tissue.<sup>35</sup> Quantitative image analysis revealed that the percentage of cells that positively immunostained for F4/80 (F4/80<sup>+</sup>) was

approximately 97% to 98% of total adherent cells (Supplemental Figure S2B). Similar results were achieved with CD68, whereas the levels of CD14<sup>+</sup> and CD206<sup>+</sup> cells were low. In contrast, CD11c<sup>+</sup> and CD34<sup>+</sup> cells were almost undetectable. These results confirm the macrophage phenotype (unpolarized) and the high purity of our unpolarized macrophage cell preparation obtained from bone marrow—derived cells. Quantitative image analysis also revealed that, similar to unpolarized macrophages, the percentage of cells that positively immunostained for F4/80 was high in both M1 and M2 cells. However, the levels of CD14<sup>+</sup> cells were high in the presence of IFN- $\gamma$  and almost undetectable in the presence of IL-4. Conversely, the levels of CD206<sup>+</sup> cells were high in the presence of IL-4 and almost undetectable in the presence of IFN- $\gamma$ . Thus, the activated, polarized phenotype of M1 cells was F4/80<sup>+</sup>/CD14<sup>+</sup>/CD206<sup>-</sup> and that of M2 cells was F4/80<sup>+</sup>/CD14<sup>-</sup>/CD206<sup>+</sup>, in agreement with previous reports.<sup>24</sup>

### PCR Experiments

Total RNA from unpolarized macrophage, M1, and M2 cells was extracted with the High Pure RNA Isolation Kit (Roche Applied Science, Mannheim, Germany), according to the manufacturer-recommended procedure. After solubilization in RNase-free water, total RNA was quantified by the Nanodrop 2000 spectrophotometer (Thermo Fisher Scientific, Waltham, MA). First-strand cDNA was generated from 1  $\mu$ g of total RNA using the ImProm-II Reverse Transcription System (Promega, Madison, WI). As shown in Table 2, a set of primer pairs, amplifying fragments ranging from 85 to 354 bp, was designed to hybridize to unique regions of the appropriate gene sequence. The PCRs were performed using 1  $\mu$ L of cDNA and the GoTaq Green Master Mix (Promega), containing 500 nmol/L of appropriate primers. The amplification reactions were performed in the MJ Mini personal thermal cycler (Bio-Rad). A sample (5  $\mu$ L) of the PCR was electrophoresed on ethidium

**Table 2** Primer Pairs Designed for PCR Analysis

Name	Symbol	Gene accession No.	Primer sequence	Amplicon (bp)	Source
TR $\alpha$	<i>Thra</i>	NM_178060	F: 5'-GGACAAAGACGAGCAGTGTGTCG-3' R: 5'-TGTGCGGCGAAAGAAGCCCT-3'	100	Custom designed
TR $\beta$ 1	<i>Thrb</i>	NM_001113417	F: 5'-CAGAAGCCCCGTCCAGACCGA-3' R: 5'-TTCAGTGCACCACGCCTCTCC-3'	101	Custom designed
CCL2	<i>Ccl2</i>	NM_011333	F: 5'-AGGTGTCCCAAAGAAGCTGTA-3' R: 5'-ATGTCTGGACCATTCTCTCT-3'	85	RTPrimerDB*
CCL5	<i>Ccl5</i>	NM_013653	F: 5'-ATATGGCTCGGACACCACCTC-3' R: 5'-GTGACAAACACGACTGCAAGA-3'	123	RTPrimerDB*
CCL9	<i>Ccl9</i>	NM_011338	F: 5'-CCCTCTCCTTCTCATTTCTTACA-3' R: 5'-AGTCTTCAAAGCCCATGTGAAA-3'	141	PrimerBank <sup>†</sup>
CD36	<i>Cd36</i>	NM_001159558 NM_007643 NM_001159555 NM_001159557 NM_001159556	F: 5'-ATGGGCTGTGATCGGAACCTG-3' R: 5'-GTCTTCCCAATAAGCATGTCTCC-3'	110	PrimerBank <sup>†</sup>
CXCL9	<i>Cxcl9</i>	NM_008599	F: 5'-TCCTTTTGGGCATCATCTTCC-3' R: 5'-TTTGTAGTGGATCGTGCCTCG-3'	110	PrimerBank <sup>†</sup>
CXCL10	<i>Cxcl10</i>	NM_021274	F: 5'-TCCTTGCTCCTCCCTAGCTCA-3' R: 5'-ATAACCCCTTGGGAAGATGG-3'	124	RTPrimerDB*
CXCL12	<i>Cxcl12</i>	NM_001012477 NM_013655 NM_021704	F: 5'-TGCATCAGTGACGGTAAACCA-3' R: 5'-TTCTTCAGCCGTGCAACAATC-3'	146	PrimerBank <sup>†</sup>
CXCL16	<i>Cxcl16</i>	NM_023158	F: 5'-CCTTGCTCTTGGGTTCTTCC-3' R: 5'-TCCAAAGTACCCTGCGGTATC-3'	139	PrimerBank <sup>†</sup>
CXCR4	<i>Cxcr4</i>	NM_009911	F: 5'-TCCAAACAAGGAACCCCTGCTTC-3' R: 5'-TTGCCGACTATGCCAGTCAAG-3'	101	RTPrimerDB*
IL-1 $\beta$	<i>Il1b</i>	NM_008361	F: 5'-GCAACTGTTCTGAACTCAACT-3' R: 5'-ATCTTTTGGGGTCCGTCAACT-3'	89	PrimerBank <sup>†</sup>
IL-10	<i>Il10</i>	NM_010548	F: 5'-GCTCTTACTGACTGGCATGAG-3' R: 5'-CGCAGCTCTAGGAGCATGTG-3'	105	PrimerBank <sup>†</sup>
IL-13	<i>Il13</i>	NM_008355	F: 5'-AGACCAGACTCCCCTGTGCA-3' R: 5'-TGGGTCCTGTAGATGGCATTG-3'	123	RTPrimerDB*
TNF- $\alpha$	<i>Tnf</i>	NM_013693	F: 5'-TTCTGTCTACTGAACTTCGGGTGATCGGTCC-3' R: 5'-GTATGAGATAGCAAATCGGCTGACGGTGTGGG-3'	354	RTPrimerDB*
GAPDH	<i>Gapdh</i>	NM_008084	F: 5'-ACCCAGAAGACTGTGGATGG-3' R: 5'-ACACATTGGGGGTAGGAACA-3'	172	RTPrimerDB*

\*Available at <http://medgen.ugent.be/rtpriimerdb/index.php>, last accessed February 26, 2013.

<sup>†</sup>Available at <http://pga.mgh.harvard.edu/primerbank>, last accessed February 26, 2013.

F, forward; GAPDH, glyceraldehyde-3-phosphate dehydrogenase; R, reverse.

bromide—containing 2.5% agarose gel by the use of the Bio-Rad Subcell GT System. After migration, bands corresponding to the amplified products were visualized with the Bio-Rad Gel Doc XR System. Real-time quantitative PCR (qPCR) was performed using a LightCycler 480 SYBR Green I Master (Roche Applied Science) on Roche LightCycler 480 Instrument, according to the manufacturer-recommended procedure. All reactions were run as triplicates. The melt-curve analysis was performed at the end of each experiment to verify that a single product per primer pair was amplified. Regarding control experiments, gel electrophoresis was also performed to verify the specificity and size of the amplified qPCR products. Samples were analyzed using the Roche LightCycler 480 Software release 1.5.0 and the second derivative maximum method. The fold increase or decrease was determined relative to a calibrator after normalizing to glyceraldehyde-3-phosphate

dehydrogenase (internal standard) through the use of the following formula:

$$2^{-\Delta\Delta C_T}^{36,37}$$

Because there is a great overlap in surface protein expression between the different macrophage subsets, we decided to quantify specific gene expression profiles.<sup>13</sup> Thus, macrophage activation obtained under our experimental protocol was confirmed by qPCR of specific patterns of cytokines and receptors. In agreement with previous reports,<sup>27</sup> M1 cells, when compared with M2 cells, expressed higher levels of transcripts encoding chemokine (C-C motif) ligand (CCL) 5 (alias RANTES, regulated upon activation, normal T cell expressed and secreted), *CXCL9* (alias monokine induced by IFN- $\gamma$ ), *CXCL10* (alias IFN- $\gamma$ -induced protein-10), *CXCL16*, *IL-1 $\beta$* , *IL-10*, and *TNF- $\alpha$*  (Supplemental Figure S3A). Conversely, M2 cells, when compared with M1, expressed higher levels of the transcripts encoding



CCL2, CCL9, the integral membrane protein CD36, the chemokine receptor CXCR4 (alias fusin or CD184), and IL-13. The melt-curve analysis and the conventional gel electrophoresis confirmed the qPCR readings (Supplemental Figure S3, B and C). These results indicate that IFN- $\gamma$ -treated cells displayed a typical M1 gene signature and IL-4-treated cells had a typical M2 gene signature.<sup>13,22–24</sup>

## Western Blot Analysis

Unpolarized macrophage, M1, and M2 cells were harvested and homogenized for 10 minutes at 4°C in radioimmunoprecipitation assay lysis buffer, containing 50 mmol/L Tris-HCl (pH 7.4), 150 mmol/L NaCl, 1% NP-40, 1% sodium deoxycholate, 1 mmol/L EDTA, 0.1% SDS, and supplemented with protease inhibitors. The supernatant was obtained by centrifugation at 2000  $\times$  g (5 minutes). When indicated, human melanoma C32 whole cell lysate (*sc-2205*) (Santa Cruz Biotechnology, Santa Cruz, CA) was used as a positive control, according to the manufacturer-recommended procedure. Protein concentration was determined using the bicinchoninic acid assay (Thermo Fisher Scientific), according to the manufacturer-recommended procedure. SDS and  $\beta$ -mercaptoethanol were added to samples before boiling, and an equal amount of proteins (40  $\mu$ g per lane) was separated by 10% SDS-PAGE with the Bio-Rad Mini-PROTEAN 3 system.<sup>38</sup> After transfer of proteins onto nitrocellulose membrane (GE Healthcare, Milan, Italy), blots were blocked for 1 hour with Tris-buffered saline–0.1% (v/v) Tween containing 5% skimmed-milk powder. The incubation with primary antibody (Table 1) was performed overnight at 4°C. After 1 to 3 hours of incubation with the appropriate horseradish peroxidase (HRP)-conjugated secondary antibody, bands were visualized using SuperSignal West Pico Chemiluminescent Substrate (Thermo Fisher Scientific), according to the manufacturer's instructions, and exposure to autoradiography Cl-Xposure films (Thermo Fisher Scientific) or with a Bio-Rad ChemiDoc MP imaging system. When indicated, alkaline phosphatase (AP)-conjugated secondary antibody was used in combination with the colorimetric AP and peroxidase substrate detection system (Sigma-Aldrich, St. Louis, MO), according to the manufacturer's instructions. To monitor potential artifacts in loading and transfer among samples in different lanes, the blots were routinely treated with the Restore Western Blot Stripping Buffer (Thermo Fisher Scientific) and reprobed with anti- $\beta$ -actin primary antibody and the appropriate HRP-conjugated secondary antibody (Table 1).

## Immunofluorescence Microscopy and Flow Cytometry of Thyroid Hormone Receptors

By using published protocols,<sup>39,40</sup> unpolarized, M1, M2, and peritoneal macrophages (see later) were cultured on glass coverslips coated with poly-L-lysine. Cells were fixed in ice-cold 4% paraformaldehyde in PBS for 5 minutes and

quenched with 1% glycine-PBS. Incubation with anti-F4/80 antibody (Table 1) was then performed in a humid chamber overnight at 4°C. Cells were then permeabilized in 0.25% Triton X-100 in PBS and incubated with anti-TR $\alpha$ 1 and anti-TR $\beta$ 1 antibodies for 2 hours before staining (1 hour) with appropriate secondary antibodies for fluorescence detection (Table 1). Nuclei were also stained with Hoechst 33258 for 5 minutes. Samples were washed in PBS and mounted on glass slides for fluorescence examination using a Leica DMI4000 B automated inverted microscope equipped with a DCF310 digital camera (Leica Microscopy Systems, Heerbrugg, Switzerland). Images were collected under a 100 $\times$  oil immersion objective. Image acquisition was controlled by Leica LAS AF software version 2.5.0.6735.

The expression of TR $\beta$ 1 on unpolarized macrophage cells was performed by flow cytometry, as previously described. Cells were incubated with anti-TR $\beta$ 1 antibody (Table 1) for 2 hours before staining (1 hour) with appropriate secondary antibodies. For intracellular staining, cells were fixed in 4% paraformaldehyde and 0.1% saponin, which were added to the antibody and wash solutions because permeabilization with saponin is reversible.

## Cell Counts

The number of viable adherent unpolarized macrophage cells was evaluated by dye exclusion (indicative of an intact membrane) using the DNA-binding probe, propidium iodide (PI) or trypan blue. Briefly, pelleted cells (unlysed) were added to PBS containing 2  $\mu$ g/mL PI and cells were counted by flow cytometry within 30 minutes. In particular, cells were acquired for a constant amount of time, using enough time to acquire at least 10,000 events for samples. Alternatively, the cell concentration was measured after 0.2% trypan blue staining by counting trypan blue-excluding cells (aliquots of 50  $\mu$ L) in a standard hemocytometer chamber under low-power microscopy.

## Apoptosis

Apoptosis was analyzed as described previously.<sup>41,42</sup> Briefly, phosphatidylserine exposure on the outer leaflet of the plasma membrane in PI-excluding cells was detected by flow cytometry of unpolarized macrophage cells (duplicate samples) stained for 15 minutes with 1  $\mu$ g/mL fluorescein isothiocyanate-labeled annexin V.

## Phagocytosis

The Phagocytosis Assay Kit (IgG fluorescein isothiocyanate) (Cayman Chemical Company, Ann Arbor, MI) was used following the manufacturer's instruction protocol. The kit uses latex beads coated with fluorescently labeled rabbit-IgG. The engulfed fluorescent beads in unpolarized macrophage, M1, and M2 cells were determined by flow cytometry at 3-hour bead exposure, when the number of M1

phagocytic cells reached the maximal values. M1 cells were also incubated with the latex beads for 1 hour (intermediate values of fluorescent-positive cells). Both the percentage of macrophages engaging in phagocytosis (percentage positive) and MFI (as a measure of the extent of fluorescence/phagocytosed latex beads) were determined. Because flow cytometry measures both beads bound to the surface and beads internalized, microscopy images on a Leica DMI4000 B automated inverted microscope equipped with a DCF310 digital camera were taken of cells after phagocytosis. After 3 hours of bead exposure, fluorescence appeared inside the M1 cells (data not shown), thus suggesting that phagocytosis had taken place. These results support that the uptake measured by flow cytometry is phagocytosis, although we cannot exclude the surface binding of beads.

### Cytokine Release

By using published protocols,<sup>27,39,43</sup> IFN- $\gamma$ , IL-13, and tumor necrosis factor (TNF)- $\alpha$  levels were measured and quantified in the culture cell supernatants by means of commercially available enzyme-linked immunosorbent assay (ELISA) kits (RayBiotech, Norcross, GA), according to the manufacturer-recommended procedure. Briefly, the supernatants of unpolarized macrophage cells were collected after 24 or 48 hours of culture, and the color intensity of the reaction product (proportional to the cytokine concentration) was quantified spectrophotometrically by the GloMax Multi detection system (Promega). Each experiment was performed in quadruplicate. At the end of each experiment, viable cells were counted with a standard hemocytometer chamber and trypan blue exclusion. Release data were expressed as pg/mL of medium/10<sup>6</sup> cells. Basal values were consistent with previous reports.<sup>27,43</sup>

### Migration Assay

The migration of unpolarized macrophage cells was assessed using Costar Transwell permeable supports (Corning Incorporated Life Sciences, Tewksbury, MA), which are chambers with inserts (8- $\mu$ m pore polycarbonate membranes). Following published protocols,<sup>44,45</sup> unpolarized macrophages were plated in the appropriate medium in the upper chamber, whereas medium with 100 ng/mL M-CSF (used as chemoattractant) was placed in the lower chamber. After 24-hour migration, nonmigratory cells were removed from the top of the insert membrane by gently wiping (cotton swabs). The underside of each membrane was fixed and stained with crystal violet, and the number of cells that migrated completely through the pores was counted per 0.1 mm<sup>2</sup> using a scored eyepiece.<sup>28</sup> From this, the total number of migrated cells was calculated.

### Hypothyroid Animals

Mice were made hypothyroid by treatment (at least 4 weeks) with the 0.02% anti-thyroidal drug, methimazole, and 0.1%

**Table 3** Serum Levels of THs and TSH in Mice, as Assessed by ELISA

Name	Unit	Euthyroid	Hypothyroid
Total T <sub>3</sub>	nmol/L	2.19 $\pm$ 0.23	0.22 $\pm$ 0.02
Total T <sub>4</sub>	nmol/L	63.19 $\pm$ 14.52	7.14 $\pm$ 3.93
TSH	mIU/L	9.43 $\pm$ 1.15	23.02 $\pm$ 5.66

sodium perchlorate in the drinking water.<sup>46</sup> The treatment was continued until the end of experiments. In agreement with previous reports,<sup>46–48</sup> classic signs of hypothyroidism, such as reduced weight compared with the untreated controls (euthyroid mice), were observed. At the end of treatment, the blood of five mice per group (euthyroid and hypothyroid) was withdrawn from eyes of anesthetized animals for the assessment of thyroid status. Briefly, total T<sub>3</sub>, total T<sub>4</sub>, and thyrotropin (TSH) in serum specimens were measured by means of triiodothyronine/thyroxine ELISA kits (Calbiotech, Spring Valley, CA) and TSH ELISA kits (Bio-Medical Assay, Beijing, China), according to the manufacturer-recommended procedure. As shown in Table 3, the hormone levels of the animals mirrored the expected values,<sup>49</sup> in agreement with other reports in mice.<sup>46,50–53</sup>

When indicated, hypothyroid mice were treated i.p. with 0.2  $\mu$ g/g body weight per day T<sub>3</sub> for 5 days, an approach used to increase the levels of circulating hormones, as previously described.<sup>47,54</sup> Hypothyroid mice were also i.p. injected with the TR antagonist, amiodarone hydrochloride (AMIO).<sup>55</sup> Each mouse received injections of AMIO at a dose of 20  $\mu$ g/g body weight per day for 2 weeks before treatment with T<sub>3</sub>, as previously described. Mice used as a control received i.p. injections of vehicle at an equivalent volume as the experimental groups. For all of the experiments and analytic methods, we used three mice per group as a minimum. All of the experiments were repeated at least three times.

### Isolation of Resident Peritoneal Cavity Cells

The peritoneal cavity is a unique compartment within which a variety of immune cells reside, and from which macrophages are commonly drawn without altering their physiological properties.<sup>56</sup> Peritoneal macrophages from euthyroid/hypothyroid mice were collected by peritoneal lavage with 5 mL ice-cold PBS supplemented with 3% FBS. The exudates were strained to remove peritoneal debris and centrifuged to isolate the cell pellet. The cell pellet was immediately resuspended in ice-cold PBS and kept on ice until immunophenotyping by flow cytometry.

### In Vivo Inflammation Experiments

As previously reported,<sup>45,57</sup> acute illness was induced by a single i.p. injection of 10 to 15  $\mu$ g/g body weight of LPS (endotoxin, *Escherichia coli* serotype O55:B5). Survival

was monitored for 96 hours. In another set of experiments, mice received a single injection i.p. of LPS for 16 hours before the isolation and flow cytometry analysis of resident peritoneal cavity cells.

## Statistics

On verification of normal distribution, statistical significance of raw data between the groups in each experiment was evaluated using the Student's *t*-test or one-way ANOVA, followed by the Newman-Keuls multiple comparison post test. Kaplan-Meier data were analyzed with the multiple comparison survival curve method using the log-rank (Mantel-Cox) test. The GraphPad Prism software package version 5.01 (GraphPad Software, San Diego, CA) was used. After statistics, data belonging from different experiments were represented and averaged in the same graph. The results were expressed as means  $\pm$  SEM of the indicated *n* values.

## Chemicals

M-CSF, IFN- $\gamma$ , and IL-4 were purchased from Miltenyi Biotec (Bergisch Gladbach, Germany).  $\alpha$ -Minimum essential medium and annexin V were obtained from Life Technologies (Monza, Italy). FBS and PBS were purchased from Euroclone (Milano, Italy). Primer pairs were obtained from Primm (Milano, Italy). The 1-850 was obtained from Santa Cruz Biotechnology. Antibodies are as follows (Table 1): CD11c, CD34, and CD206 (BioLegend, San Diego, CA), CD14 (BD Biosciences, Franklin Lakes, NJ), CD68 and F4/80 (Acris Antibodies, Herford, Germany), TR $\beta$  (*ab53170*) (Abcam, Cambridge, UK), TR $\alpha/\beta$  (*sc-772*), TR $\alpha1$  (*sc-10819*), TR $\beta1$  (*sc-738*), and arginase 1 (*sc-20150*) (Santa Cruz Biotechnology),  $\beta$ -actin (*A5441*) (Sigma-Aldrich), HRP-anti-rabbit (Cell Signaling, Danvers, MA), AP-anti-rabbit (Promega), HRP-anti-mouse (Bio-Rad), and Alexa Fluor 456 anti-goat/mouse/rabbit (Life Technologies). When appropriate, all reagents and solutions were verified to be endotoxin free by the Sigma Limulus amoebocyte lysate assay (sensitivity limit, 0.1 ng/mL). Where not specified, chemicals and reagents were purchased from Sigma-Aldrich.

## Results

### TR Expression in Unpolarized Macrophage Cells

The major isoforms, TR $\alpha1$  and TR $\beta1$ , are bona fide receptors to which T<sub>3</sub> binds with high affinity.<sup>7</sup> TRs were found to be widely expressed throughout the body, including in immune and hematopoietic cells.<sup>7,11,12,26,58–61</sup> As shown in the PCR experiments of Figure 1A, primary cultures of unpolarized macrophage cells express detectable mRNA levels of TR $\alpha$  and TR $\beta1$ . In addition, as depicted in Western blot experiments with anti-TR $\alpha/\beta$  antibody (Figure 1B), using C32 cell proteins

as a positive control, we detected two immunoreactive bands corresponding to the molecular weights of TR $\alpha1$  (47 kDa) and TR $\beta1$  (52 kDa). In contrast, we detected only the TR $\beta$ -specific band in unpolarized macrophage cells. In another set of experiments, immunofluorescence analysis of unpolarized macrophage cells with anti-TR $\alpha1$  and anti-TR $\beta1$  antibodies, in combination with an anti-F4/80 antibody (a macrophage-specific surface marker) and Hoechst staining, allowed us to study the expression of TRs at the cellular level. In broad

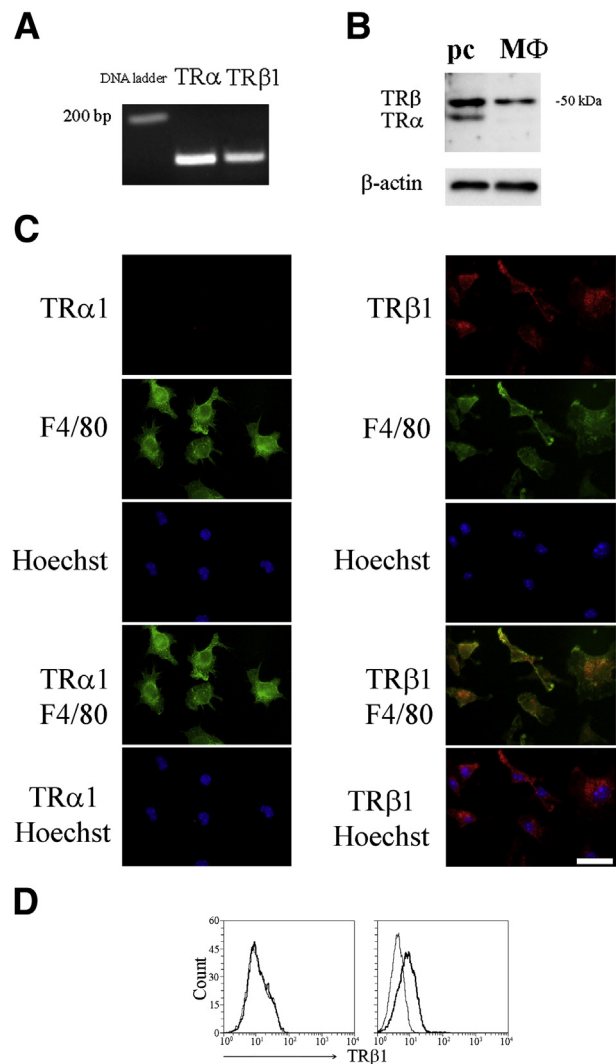


**Figure 1** TR expression in unpolarized macrophage (MΦ) cells. **A:** PCR products of distinct TR mRNAs in unpolarized macrophage cells after 8 days of culture. The panel is representative of four independent experiments. **B:** Western blot analysis of TR expression performed with the anti-TR $\alpha/\beta$  (*sc-772*) antibody.  $\beta$ -Actin (anti- $\beta$ -actin *A5441*) was used as an internal standard. The image is representative of four independent experiments. pc, positive control. **C:** Immunofluorescence analysis of unpolarized macrophage cells with anti-TR $\alpha1$  (*sc-10819*) and anti-TR $\beta1$  (*sc-738*) antibodies (red). Unpolarized macrophage cells were also stained with the anti-F4/80 antibody (green) and with Hoechst dye (blue). The images are representative of three independent experiments. Scale bar = 20  $\mu$ m. **D:** Flow cytometry analysis of TR $\beta1$  (*sc-738*) expression in unpolarized macrophage cells either left intact (**left panel**) or permeabilized (**right panel**). Results are representative of three independent experiments.

agreement with Western blot analysis, we did not find a TR $\alpha$ -specific signal (Figure 1C). Conversely, the immunostaining for TR $\beta$ 1 showed bright cytoplasmic/perinuclear labeling, whereas nuclear staining was scarce and diffuse. A similar expression pattern of TR $\beta$ 1 staining has been already demonstrated in mouse dendritic cells.<sup>11</sup> As shown in the analysis of TR $\beta$ 1 expression by flow cytometry (Figure 1D), no signal was detected in intact unpolarized macrophage cells, whereas permeabilized cells exhibited specific staining for TR $\beta$ 1, further confirming the intracellular distribution of this molecule.

### Inhibitory Effects of T<sub>3</sub> on Macrophage Differentiation

To investigate the role of THs in the physiological characteristics of macrophages, and their influence on macrophage development, we investigated whether T<sub>3</sub> affects the differentiation of monocytes into unpolarized macrophages. T<sub>3</sub> was applied daily beginning from the isolation of bone marrow-derived cells. In agreement with previous *in vitro* studies on brain macrophages,<sup>47</sup> T<sub>3</sub> was added at a final concentration of 500 nmol/L, which is a supraphysiological concentration in mouse,<sup>50–52</sup> (Table 3) giving maximal TR $\alpha$ /

TR $\beta$  occupancy.<sup>62</sup> As shown in Figure 2, A and B, after 8 days of continuous T<sub>3</sub> application, the number of adherent viable cells decreased by almost 35% and 44% versus control cells, as assessed by the trypan blue and PI exclusion tests, respectively. Actions of thyroid hormone that are not initiated by binding of the hormone to intranuclear TRs are termed nongenomic.<sup>63</sup> Plasma membrane-initiated actions begin at a receptor on integrin  $\alpha$ V $\beta$ 3. Tetrac is a TH analogue that inhibits binding of iodothyronines to the integrin receptor and is a probe for the participation of this receptor in cellular actions of the hormone.<sup>30,63,64</sup> The simultaneous application of 500 nmol/L tetrac and T<sub>3</sub> did not modify T<sub>3</sub> effects on the number of adherent viable cells, whereas the addition of 1  $\mu$ mol/L TR antagonist 1-850<sup>65–67</sup> inhibited T<sub>3</sub> actions (Figure 2A). In addition, T<sub>3</sub> effects were dependent on the time of exposure (Figure 2B). The absence of phosphatidylserine exposure on the outer leaflet of the plasma membrane, measured by annexin V staining, excluded the induction of apoptosis during T<sub>3</sub> exposure (Supplemental Figure S4). Similarly, flow cytometry analysis revealed that T<sub>3</sub> reduced the expression of the pan-macrophage markers F4/80 and CD68 and the number of F4/80<sup>+</sup> cells in the population of adherent cells (Figure 2, C and D), suggesting that not

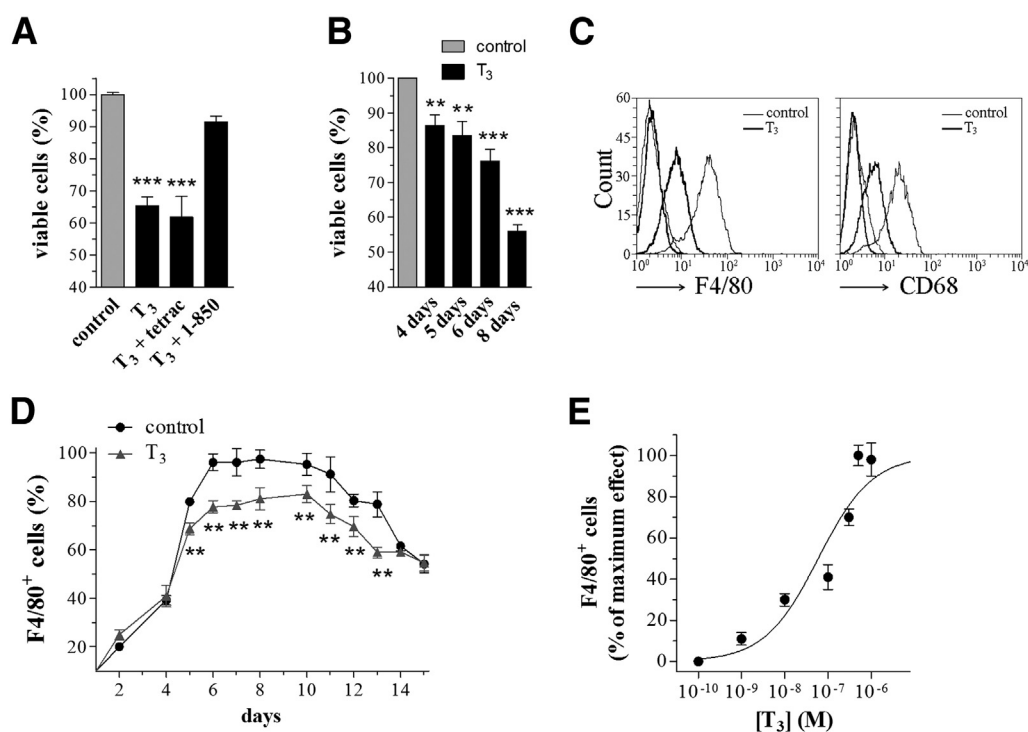


**Figure 2** T<sub>3</sub> and differentiation of unpolarized macrophage cells. **A:** Bone marrow-derived cells were differentiated into unpolarized macrophages in the absence (control) or in the presence of 500 nmol/L T<sub>3</sub>, 500 nmol/L tetrac, or 1  $\mu$ mol/L 1-850. Cell viability was measured after 8 days of culture by counting vital cells (trypan blue exclusion test). Data are expressed by setting the control as 100%. Each histogram represents the means  $\pm$  SEM of data from five independent experiments. **B–D:** Bone marrow-derived cells were differentiated into unpolarized macrophages in the absence (control) or in the presence of 500 nmol/L T<sub>3</sub>. **B:** PI exclusion test (cell counting) by flow cytometry at different days of culture. Each histogram represents the means  $\pm$  SEM of data from five independent experiments. Data are expressed by setting the control as 100%. **C:** Cell surface analysis by flow cytometry of F4/80 and CD68 expression after 8 days of culture. Results are representative of three to five independent experiments. **D:** F4/80-positive cells analyzed by flow cytometry at different days of culture. Each point represents the means  $\pm$  SEM of data from five independent experiments. Data are expressed by setting as 100% the total adherent cells at each time point. **E:** Bone marrow-derived cells were differentiated into unpolarized macrophages in the presence of increasing concentrations of T<sub>3</sub>. Concentration-response curve of T<sub>3</sub> effects on the number of F4/80<sup>+</sup> cells (by flow cytometry) at 8 days of culture. Each point represents the means  $\pm$  SEM of data from three independent experiments. Data are expressed by setting as 100% the maximum effect of T<sub>3</sub>. \*\**P* < 0.01, \*\*\**P* < 0.001 versus respective control.



all of the living cells that are adherent to the substrate had differentiated into macrophages. The fact that the levels of CD34 and CD11c markers were almost undetectable in both control and T<sub>3</sub>-exposed cells (data not shown) demonstrates the virtual absence of hematopoietic- and dendritic-like phenotypes, although we cannot exclude that, in the presence of the hormone, progenitor cells may differentiate toward other lineages. Collectively, these data indicate that a bone marrow-derived cell suspension differentiates into a population of living cells expressing macrophage markers mostly between days 4 and 8, and that T<sub>3</sub> affects the ability of cells to attach and, thus, to completely differentiate to macrophages.

The concentration used in these *in vitro* experiments is higher than the T<sub>3</sub> serum concentration achieved in our *in vivo* models (Table 3); thus, we tested if the observed inhibitory effects of T<sub>3</sub> exposure on F4/80<sup>+</sup> cells were concentration dependent and if they are detectable at concentrations of T<sub>3</sub> comparable with the physiological serum concentration. As shown in Figure 2E, T<sub>3</sub> application caused a concentration-dependent effect on F4/80<sup>+</sup> cells (EC<sub>50</sub> = 59 nmol/L). No significant effects were seen with concentrations <10 nmol/L, whereas the maximal changes were seen with concentrations >300 nmol/L.

### Effects of T<sub>3</sub> on Differentiated Macrophage Cells

We investigated whether 500 nmol/L T<sub>3</sub> affected only unpolarized macrophage differentiation or acted also on differentiated macrophages. Cells were treated with T<sub>3</sub> for 24 hours after bone marrow-derived cell differentiation (8 days) onto macrophage cells. As shown in Figure 3A, in macrophage cells, the mRNA levels of TR $\alpha$  were not modified by T<sub>3</sub>, whereas the hormone decreased the expression of TR $\beta$ 1 mRNA. In addition, T<sub>3</sub> decreased the expression of the TR $\beta$  protein band, as confirmed by using Western blot analysis using an anti-TR $\beta$ -specific antibody (Figure 3B).

The number of adherent viable cells was not affected by T<sub>3</sub> application, as assessed by the PI exclusion test (Figure 3C). Remarkably, flow cytometry analysis revealed that T<sub>3</sub> increased the percentage of F4/80/CD14 (M1 marker)-positive cells by almost 50% (Figure 3D) and increased the levels of transcripts (Figure 3E) encoding for genes selectively expressed by M1-activated macrophages (as described in Materials and Methods). In addition, T<sub>3</sub> decreased the expression of genes selectively expressed by M2-activated macrophages, whereas the percentage of F4/80/CD206 (M2 marker)-positive cells remained undetectable (data not shown). Consistently, T<sub>3</sub> increased the release in the supernatant of the M1 cytokines, IFN- $\gamma$  and TNF- $\alpha$  (Table 4). This effect was registered 48 hours after T<sub>3</sub> application, but not after 24 hours. Accordingly, in mouse macrophages *in vitro*, application of T<sub>3</sub> and T<sub>4</sub> at supraphysiological concentrations for 24 hours was found to be devoid of effects on cytokine release, including TNF- $\alpha$ .<sup>20</sup> Herein, we also show that the release of the M2 cytokine, IL-13, was not affected by T<sub>3</sub>.

Interestingly, T<sub>3</sub> also inhibited the migratory ability of macrophages by almost 37% (Figure 3F).

### T<sub>3</sub> Regulates Macrophage Activation toward M1/M2

Macrophages were activated into polarized M1 or M2 via exposure to IFN- $\gamma$  for 2 days or M-CSF + IL-4 for 4 days, respectively.<sup>27,28</sup> As detailed in Materials and Methods, the specificity of polarization was assessed by flow cytometry using various surface markers characterizing the various cell

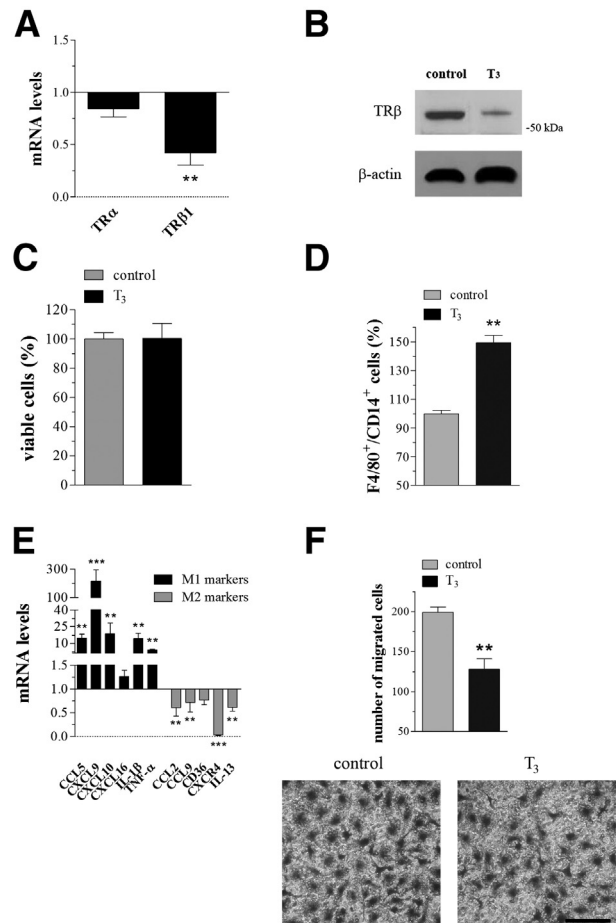


**Figure 3** T<sub>3</sub> and differentiated macrophage cells. Macrophage cells were treated in the absence (control) or in the presence of 500 nmol/L T<sub>3</sub> for 24 hours. **A:** qPCR of TR mRNAs in the presence of T<sub>3</sub>. Values are expressed as means  $\pm$  SEM ( $n = 9$ ) of the fold change over control (set as 1). **B:** Western blot analysis of TR $\beta$  protein (anti-TR $\beta$  ab53170).  $\beta$ -Actin (anti- $\beta$ -actin A5441) was used as an internal standard. The image is representative of five independent experiments. pc, positive control. **C** and **D:** PI exclusion test (cell counting) and analysis of F4/80/CD14-positive cells, respectively, by flow cytometry. Each histogram represents the means  $\pm$  SEM of data from 10 independent experiments. Data are expressed by setting the control as 100%. **E:** qPCR of mRNAs encoding for genes selectively expressed by M1 or M2 activated cells, in the presence of T<sub>3</sub>. Values are expressed as means  $\pm$  SEM ( $n = 4$ ) of the fold change over control (set as 1). **F:** The number of migrated cells is plotted for each experimental condition (using 100 ng/mL M-CSF as chemoattractant) (**top panel**). Each histogram represents the means  $\pm$  SEM of data from five independent experiments. Representative stains of migrated cells are depicted (**bottom panel**). Scale bar = 40  $\mu$ m. \*\* $P < 0.01$ , \*\*\* $P < 0.001$  versus respective control.

**Table 4** Concentrations of Soluble Molecules in the Supernatants of Macrophages, as Assessed by ELISA

Name	At 24 hours	At 48 hours
IFN- $\gamma$		
Control	12.77 $\pm$ 1.03	14.20 $\pm$ 0.70
T <sub>3</sub>	11.86 $\pm$ 0.81	28.26 $\pm$ 3.93*
IL-13		
Control	ND	ND
T <sub>3</sub>	ND	ND
TNF- $\alpha$		
Control	129.9 $\pm$ 11.20	176.3 $\pm$ 17.06
T <sub>3</sub>	131.7 $\pm$ 11.38	293.2 $\pm$ 54.73*

Values are given in pg/mL  $\times$  10<sup>6</sup> cells.

\**P* < 0.05 versus respective control.

ND, not detectable.

subsets and gene expression profiles of specific patterns of cytokines and receptors. Then, the relative expression of TRs in unpolarized macrophage, M1, and M2 cells was investigated. As shown in Figure 4A, the transcript encoding TR $\alpha$  was similarly expressed by both unpolarized and polarized cells, whereas the expression of TR $\beta$  mRNA was enhanced in M2 cells (approximately 25 fold versus unpolarized macrophages) but not in M1. As depicted in Western blot experiments with anti-TR $\alpha/\beta$  antibody (Figure 4B), we detected only the TR $\beta$ -specific band in M1 and M2 cells, which appeared to be up-regulated in M2 when compared with unpolarized macrophage cells. In addition, immunofluorescence analysis with anti-TR $\alpha$ 1 and anti-TR $\beta$ 1 antibodies, in combination with the anti-F4/80 antibody and Hoechst staining, showed the absence of TR $\alpha$ 1-specific signal in M1 (Figure 5A) and M2 (Figure 5B) cells. In contrast, strong perimembranous and cytoplasmic/perinuclear labeling for TR $\beta$ 1 was found in both cell models. The nuclear staining for TR $\beta$ 1 was generally scarce and diffuse.

In another set of experiments, T<sub>3</sub> was administered at 500 nmol/L to unpolarized macrophages daily, starting from the beginning of the activation process. When combined with M1 stimulation, T<sub>3</sub> significantly increased the number of F4/80<sup>+</sup> also positive for CD14, while not affecting the overall percentage of F4/80-positive cells (Figure 6A). T<sub>3</sub> exposure differentially modulated the expression of M1 marker genes. In particular, it increased the expression of CXCL16 and TNF- $\alpha$  mRNAs, whereas, unexpectedly, it decreased the levels of transcripts encoding CCL5 and IL-1 $\beta$  (Figure 6C). When combined with M2 stimulation, T<sub>3</sub> significantly decreased the number of F4/80<sup>+</sup> also positive for CD206, while not affecting the overall percentage of F4/80-positive cells (Figure 6B). Consistently, T<sub>3</sub> decreased the expression of the M2 marker genes, *CCL2*, *CCL9*, *CD36*, and *IL-13* (Figure 6C).

Arginase 1, a manganese metalloenzyme that catalyzes the hydrolysis of L-Arg to L-ornithine and urea, is one of the most specific markers of M2 macrophages.<sup>68–70</sup> M2 activation led to a marked up-regulation of arginase 1 that was inhibited by treatment with 500 nmol/L T<sub>3</sub> (Figure 7A).

We finally assessed the effect of 500 nmol/L T<sub>3</sub> at the functional level. To this end, we relied on phagocytosis, which is increased in M1 cells compared with unpolarized or M2 macrophages.<sup>28</sup> Phagocytosis was measured using latex beads coated with fluorescently labeled IgG, by determining, in flow cytometry analyses, the percentage of positive (ie, actively phagocytosing) cells and the extent of phagocytosis as MFI. As shown in Figure 7B, phagocytic M2 cells were 28% less than M1 cells and the extent of phagocytosis in M1 cells was 3.9-fold higher than that of M2 cells. Of interest, T<sub>3</sub> increased both the percentage of M1 cells participating in phagocytosis and the extent of phagocytosis (Figure 7C).

### T<sub>3</sub> Affects Macrophage Subsets *in Vivo*

We investigated whether the sensitivity of macrophages to T<sub>3</sub>, determined in *in vitro* experiments, was observed *in vivo*. Immunofluorescence analysis with anti-TR $\alpha$ 1 and anti-TR $\beta$ 1 antibodies, in combination with the anti-F4/80 antibody and Hoechst staining, showed the substantial

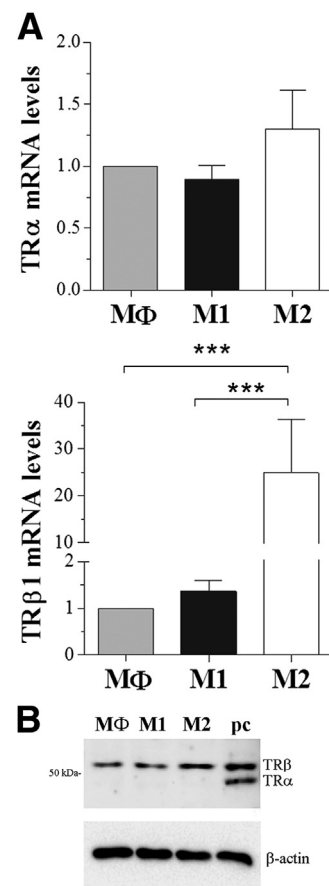


**Figure 4** TR expression in unpolarized macrophages (M $\Phi$ ), M1, and M2 cells. **A:** qPCR of mRNAs encoding for TR $\alpha$  and TR $\beta$ 1 genes. Values are expressed as means  $\pm$  SEM (*n* = 3 to 5) of the fold change over unpolarized macrophages (set as 1). \*\*\**P* < 0.001. **B:** Western blot analysis performed with the anti-TR $\alpha/\beta$  (sc-772) antibody.  $\beta$ -Actin (anti- $\beta$ -actin A5441) was used as internal standard. The image is representative of four independent experiments. pc, positive control.

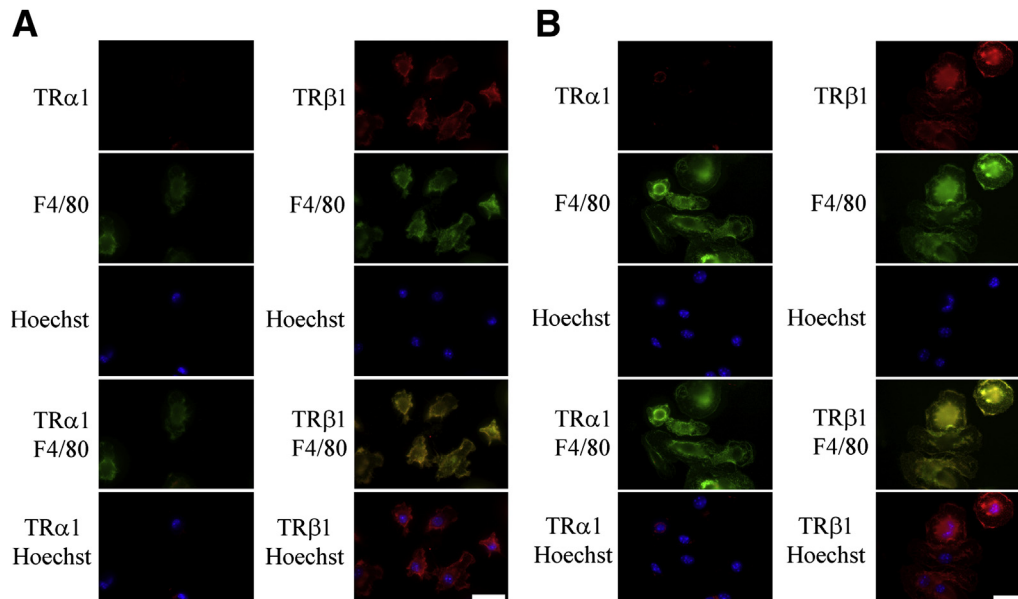


**Figure 5** Immunofluorescence analysis of TR expression in M1 (A) and M2 (B) cells stained with anti-TR $\alpha$ 1 (*sc-10819*) and anti-TR $\beta$ 1 (*sc-738*) antibodies (red). M1 and M2 cells were also stained with anti-F4/80 antibody (green) and with Hoechst dye (blue). The images are representative of three independent experiments. Scale bars: 20  $\mu$ m.

absence of TR $\alpha$ 1-specific signal in macrophages isolated from the peritoneal cavity (Figure 8). In contrast, we found strong perimembranous and cytoplasmic/perinuclear labeling for TR $\beta$ 1, whereas the nuclear staining was generally scarce and diffuse.

Then, we took advantage of an established model of hypothyroid mice (Table 3) that was compared with euthyroid mice. As shown in Figure 9A, quantitative image analysis, by flow cytometry, of isolated peritoneal cavity cells revealed similar levels of cells that positively immunostained for F4/80 in both euthyroid and hypothyroid mice; a small, but not significant, decrease of F4/80<sup>+</sup> cells was obtained after i.p. injection of hypothyroid animals with 0.2  $\mu$ g/g body weight per day T<sub>3</sub> for 5 days. These results suggest that T<sub>3</sub> levels do not perturb drastically the total content of peritoneal macrophages. Two coexisting peritoneal macrophage subsets have been recently distinguished in mice, with unique phenotypic and functional characteristics.<sup>56,71</sup> The ones expressing high levels of F4/80 (F4/80<sup>high</sup>) were defined as large peritoneal macrophages (LPMs), and the subset of remaining macrophages expressing low levels of F4/80 (F4/80<sup>low</sup>) was defined as small peritoneal macrophages (SPMs). By using the gating strategy reported in Figure 9B, we identified such different subsets of macrophages (SPM, 10.9%  $\pm$  2.5%; and LPM, 42.0%  $\pm$  3.8% versus total cell number;  $n$  = 8). In hypothyroid mice, the SPM population became the dominant macrophage subset (41.2%  $\pm$  5.9%;  $n$  = 10;  $P$  < 0.0001 versus euthyroid) and LPM frequencies decreased (11.9%  $\pm$  1.7%;  $n$  = 10;  $P$  < 0.0001 versus euthyroid). At 5 days, 0.2  $\mu$ g/g body weight per day T<sub>3</sub> i.p. injection prevented the effect of hypothyroidism on the SPM subset (12.1%  $\pm$  0.4%;  $n$  = 5;  $P$  < 0.0001 versus hypothyroid), and a slight,

but significant, effect was achieved on LPM frequencies (19.6%  $\pm$  2.9%;  $n$  = 5;  $P$  < 0.05 versus hypothyroid). In both euthyroid and hypothyroid animals, we also found that a few (<8%) of the F4/80-positive cells expressed CD14 or CD206 (data not shown).

### TH Levels Affect Animal Mortality and Peritoneal Macrophage Subsets during Endotoxemia

LPM and SPM differ markedly in their *in vivo* responses to inflammatory stimuli,<sup>56</sup> and M1 cells (CD14<sup>+</sup>) have a classic proinflammatory profile; we evaluated whether alterations of TH levels affected the animal survival rate during systemic inflammation. To this end, we injected euthyroid and hypothyroid mice i.p. with LPS to induce endotoxemia, and we recorded the mortality of the animals over 96 hours. As shown in the Kaplan-Meier curve of Figure 10A, hypothyroid mice exhibited significantly increased mortality during the course of the experiment (10% survival of hypothyroid mice versus 35% survival of euthyroid mice). When injected i.p. with 0.2  $\mu$ g/g body weight per day T<sub>3</sub> for 5 days before the onset of endotoxemia, hypothyroid animals were significantly protected from death (70% survival). To verify the involvement of TRs, hypothyroid mice were also injected i.p. with 20  $\mu$ g/g body weight per day AMIO for 2 weeks before the treatment with T<sub>3</sub> and the onset of endotoxemia. AMIO is an antiarrhythmic drug that acts *in vitro* and *in vivo* as a TR $\alpha$ 1 and TR $\beta$ 1 antagonist via its major metabolite, desethylamiodarone.<sup>55</sup> It has been recently reported that mice injected i.p. with 80  $\mu$ g/g body weight per day AMIO for 25 days had only mild alterations in TH economy, with doubling of plasma TSH concentrations in the face of steady plasma T<sub>4</sub> and T<sub>3</sub> levels.<sup>51</sup> As shown in Figure 10A, the

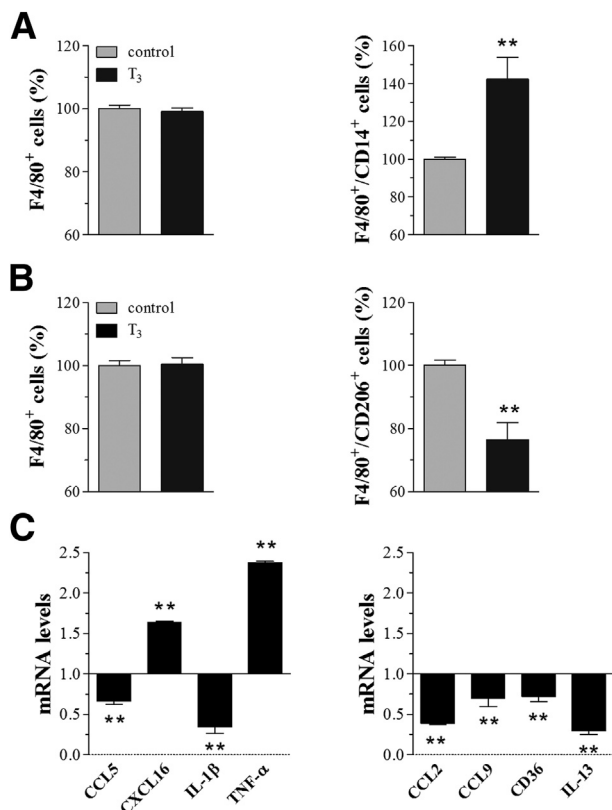


**Figure 6** T<sub>3</sub> and activation of M1/M2 cells. Macrophages were polarized into M1 or M2 in the absence (control) or in the presence of 500 nmol/L T<sub>3</sub>. **A** and **B**: Flow cytometry analysis of F4/80-positive cells and F4/80/CD14- or F4/80/CD206-positive cells in M1- and M2-stimulating conditions, respectively. Each histogram represents the means  $\pm$  SEM of data from four to six independent experiments. Data are expressed by setting the control as 100%. **C**: qPCR of mRNAs encoding for M1 or M2 genes in M1- or M2-stimulating conditions (**left** and **right** panels, respectively), and in the presence of T<sub>3</sub>. Values are expressed as means  $\pm$  SEM ( $n = 4$ ) of the fold change over control (set as 1). \*\* $P < 0.01$  versus respective control.

protective effects of T<sub>3</sub> in our system were decreased in AMIO-injected mice (45% survival).

We next delineated TH/macrophage phenotype interactions during systemic inflammation, using euthyroid and hypothyroid mice. Animals were treated i.p. with LPS for 16 hours (ie, a time interval before animal death). As previously suggested in a model of mouse injury obtained by cecal ligation and puncture,<sup>72</sup> it is likely during this period that inflammatory changes differentiate between mice that live and die. At the end of the experiment, the phenotype of peritoneal F4/80<sup>+</sup> cells was determined. In euthyroid animals, a marked shift in the SPM/LPM ratio (SPM, 37.8%  $\pm$  3.9%; LPM, 15.0%  $\pm$  1.7%;  $n = 4$ ;  $P < 0.001$  versus untreated euthyroid) was observed after LPS i.p. injection (Figure 10B). It was previously demonstrated that significantly lower doses of LPS (10  $\mu$ g versus 10 to 15  $\mu$ g/g body weight, as in our experiments) did not change mouse SPM and LPM frequencies at 20 hours after i.p. LPS injection, whereas by 2 days after stimulation, SPM becomes the highly dominant subset.<sup>56</sup> Taken together, these results indicate a correlation between LPS doses and

time-response of macrophage phenotype. As shown in Figure 10B, we also found that hypothyroid mice showed an additional increase of the SPM frequencies (58.6%  $\pm$  3.3%;  $n = 3$ ;  $P < 0.05$  versus LPS-injected euthyroid mice), whereas LPM frequencies did not substantially change (19.82%  $\pm$  2.7%) compared with LPS-injected euthyroid mice. In contrast, hypothyroid mice i.p. injected for 5 days with 0.2  $\mu$ g/g body weight per day T<sub>3</sub> and treated with LPS showed a dramatic decrease of the SPM/LPM ratio (SPM, 27.4%  $\pm$  6.7%; LPM, 35.2%  $\pm$  4.5%;  $n = 3$ ;  $P < 0.05$  versus both LPS-injected euthyroid and hypothyroid mice). After LPS injections, F480<sup>+</sup>/CD14<sup>+</sup> expression in SPM or LPM cells did not change in euthyroid, hypothyroid, or hypothyroid mice treated with T<sub>3</sub> (Figure 10C), whereas the presence of F4/80-positive cells expressing CD206 was almost undetectable (data not shown).

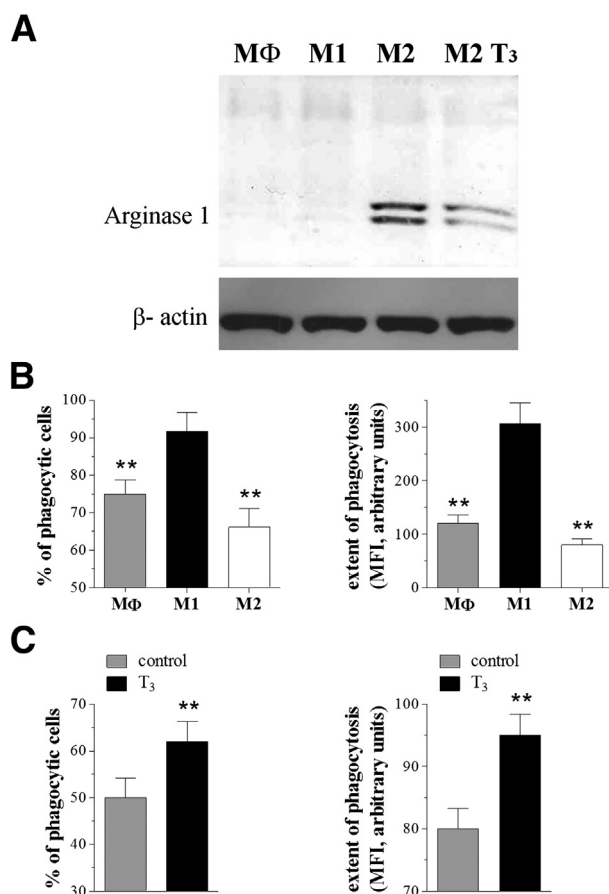


**Figure 7** **A**: Western blot analysis of arginase 1 (anti-arginase 1 sc-20150) in unpolarized macrophage, M1, and M2 cells and in the M2-stimulating condition in the presence of 500 nmol/L T<sub>3</sub>.  $\beta$ -Actin (anti- $\beta$ -actin A5441) was used as internal standard. The image is representative of three independent experiments. **B**: Percentage of phagocytic cells and MFI in unpolarized macrophage, M1, and M2 cells after 3 hours of incubation with latex beads coated with fluorescently labeled IgG. Each histogram represents the means  $\pm$  SEM of data from five independent experiments. **C**: Percentage of phagocytic cells and MFI in M1-stimulating conditions and in the presence of 500 nmol/L T<sub>3</sub>, at 1 hour of bead exposure. Each histogram represents the means  $\pm$  SEM of data from five independent experiments. \*\* $P < 0.01$  versus M1 or respective control.



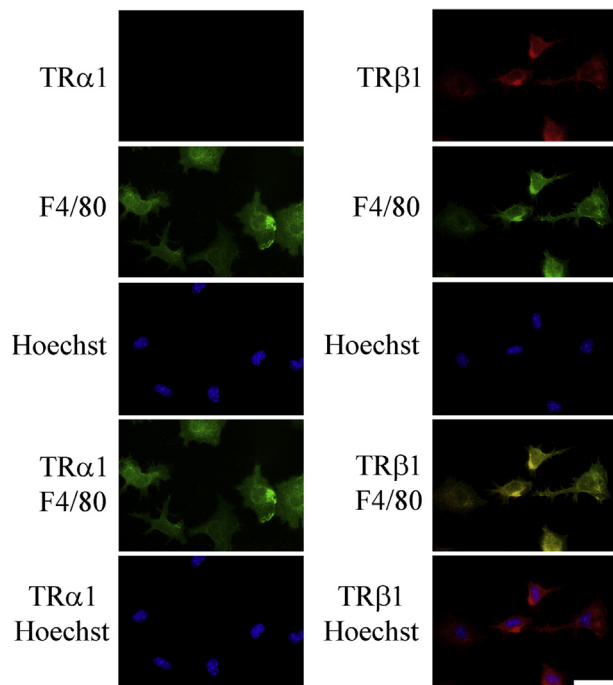


**Figure 8** Immunofluorescence analysis of TR expression in peritoneal macrophages stained with anti-TR $\alpha$ 1 (*sc-10819*) and anti-TR $\beta$ 1 (*sc-738*) antibodies (red). Macrophages were also stained with anti-F4/80 antibody (green) and with Hoechst dye (blue). The images are representative of three independent experiments. Scale bar = 20  $\mu$ m.

## Discussion

This study identifies a homeostatic link between THs and the pathophysiological role of macrophages. Macrophages fulfill key functions in immunity, and these properties may change in response to the variable microenvironmental signals of the local milieu.<sup>13,14,22</sup> There is evidence that T<sub>3</sub> drives maturation and signaling of dendritic cells,<sup>11,12</sup> the cells most closely associated with macrophages.<sup>13</sup> We show that T<sub>3</sub> affects macrophage phenotype and function, thus extending the role of this hormone as an immune-regulating factor.

### *In Vitro* Results

Bone marrow–derived monocytes enter peripheral blood and circulate for several days in an inert state before entering tissues and differentiating into tissue-resident macrophages. The endocrine system participates in regulating their differentiation and maturation.<sup>5,7,3,74</sup> Our results indicate a negative role of T<sub>3</sub> in triggering the differentiation of monocytes into macrophages in culture. Physiological concentrations of T<sub>3</sub> were suggested to regulate the cell population growth of human hematopoietic cells.<sup>58</sup> Compared with the serum concentration of T<sub>3</sub> measured in euthyroid mice<sup>50–52</sup> (present results), and disregarding any degradation during the culture time, the T<sub>3</sub> concentration used under our experimental condition *in vitro* (500 nmol/L) is higher than the physiological range. In mouse

macrophages *in vitro*, T<sub>3</sub> was recently shown to be active at supraphysiological concentrations (100 nmol/L).<sup>20</sup> In addition, tissues derive most of their T<sub>3</sub> from local de-iodination of T<sub>4</sub> and cells can regulate their T<sub>3</sub> content by means of active transport.<sup>7,8</sup> Thus, defining the exact concentration of active T<sub>3</sub> acting locally on tissue cells versus the one measured in the serum is difficult. In addition, although cell cultures mimic the *in vivo* systems, the more vigorous metabolism *in vitro* can degrade T<sub>3</sub> rapidly, dramatically reducing the initial dose after 24 hours, as described in primary cultures of rat brain cells.<sup>75</sup> Consistently, a wide range of hormone concentrations has been used *in vitro* to define the actions of THs. Several reports describe T<sub>3</sub> effects at subnanomolar-nanomolar concentrations in cell cultures,<sup>11,12,21,58,65,76–79</sup> whereas others used T<sub>3</sub> concentration of two to three orders of magnitude higher than the one measured in the serum.<sup>30,47,64,80–84</sup> As previously shown, the binding affinity curves of T<sub>3</sub> at TRs *in vitro* indicate that the maximal receptor occupancy occurs at a higher than physiological hormone concentration (ie, >10 nmol/L).<sup>62</sup> We demonstrate herein that concentrations of T<sub>3</sub> comparable with free serum concentration were not sufficient to elicit detectable effects in *in vitro* primary cultures of monocytes/macrophages, and maximal T<sub>3</sub> effects were achieved only at higher levels, as already reported in other systems, including macrophages.<sup>47,80,84</sup>

An important conclusion of our study is the demonstration that T<sub>3</sub> induces unpolarized macrophage cells to display a classically activated (M1) signature, as revealed by the expression analysis of surface proteins, gene markers, and cytokine release. Chemotaxis represents an important function by which macrophages confront certain pathogens. The motility *in vitro* of mouse M1 cells was reported to be lower than that of M2 cells<sup>28</sup>; our observation that T<sub>3</sub> induced inhibition of unpolarized macrophage migratory ability is consistent with an M1-priming effect of T<sub>3</sub>. This is also observed on activated, polarized macrophages. Indeed, we show that T<sub>3</sub> reversed M2 activation while enhancing that of M1 cells, even at a functional level. Macrophages are strategically located throughout the body tissues, where they ingest and process foreign materials, dead cells, and debris.<sup>85</sup> Our results indicating a positive fine-tuning role for T<sub>3</sub> in promoting the phagocytic activity of M1 cells are consistent with evidence that phagocytosis is increased in M1 cells compared with M2 macrophages<sup>28</sup> (present results) and with earlier observations in mice.<sup>19</sup> Different results have been reported in hypothyroid rats.<sup>16</sup> In particular, incubation *in vitro* of mouse peritoneal macrophages with higher than physiological concentrations of T<sub>3</sub> induced no modifications in the phagocytic capacity, whereas phagocytosis was stimulated by physiological concentrations of T<sub>4</sub>.<sup>17</sup> In a recent study, high concentrations of T<sub>3</sub> and T<sub>4</sub> stimulated bacterial phagocytosis of mouse macrophages.<sup>20</sup> Accordingly, *in vivo* T<sub>4</sub> treatment of mice induced a slight increase in peritoneal macrophage phagocytosis.<sup>18</sup> As previously suggested,<sup>6</sup> it is possible that the different responses

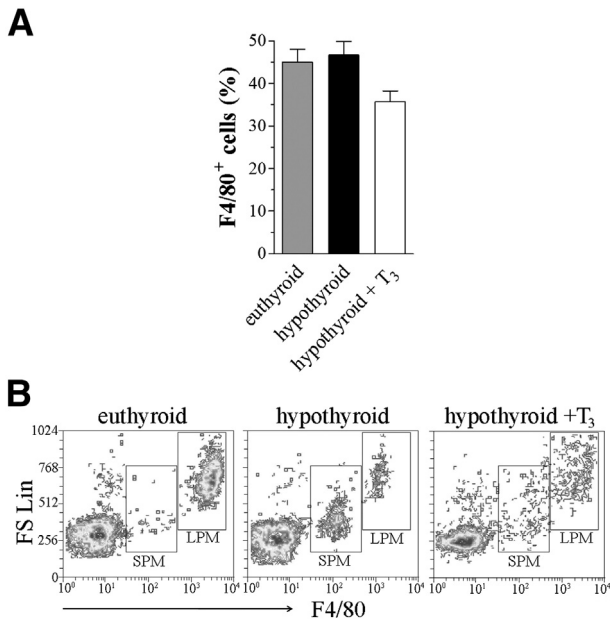


**Figure 9** T<sub>3</sub> and *in vivo* content of murine peritoneal macrophages. Cell surface analysis by flow cytometry of isolated peritoneal cavity cells in euthyroid and hypothyroid mice, as well as in hypothyroid mice injected i.p. for 5 days with 0.2 μg/g body weight per day T<sub>3</sub>. **A:** Analysis of F4/80-positive cells. Data are expressed by setting as 100% the total cell number (*n* = 8 to 18). **B:** Gating strategy used to identify the macrophage subsets of large cells expressing high levels of F4/80 (LPM) and small cells expressing low levels of F4/80 (SPM). FSLin, forward scatter in linear mode (cell size) (*n* = 5 to 10).

elicited by THs depend on the type of inert particles phagocytosed. In this respect, in our experiments, we assayed the engulfment of IgG-labeled particles; however, the effects of THs on other forms of phagocytosis (eg, the noninflammatory complement-mediated phagocytosis) would deserve further systematic investigation. It is generally assumed that M1 or M2 activation *in vivo* represents extremes of a continuum in a universe of activation states and mixed phenotypes, and coexistence of cells in different activation states has been observed in preclinical/clinical conditions.<sup>22</sup> Our data reporting the inhibition of leading M1 gene markers, such as IL-1β or CCL5, after T<sub>3</sub> exposure revealed a somehow mixed phenotype. The switching induced by T<sub>3</sub> in activated cells appears, therefore, complex and represents an important biological issue that needs to be investigated further.

The use of T<sub>3</sub> antagonists in our system indicated that T<sub>3</sub> effects are initiated by intracellular TRs. Among TRs, we found that bone marrow-derived unpolarized macrophage, M1, and M2 cells expressed detectable levels of transcripts encoding for TRα and TRβ1, the latter being positively regulated during M2 activation. The mRNAs for TRα and TRβ were previously detected in bone marrow-derived macrophages and found to increase in IFN-γ-primed cells.<sup>26</sup> However, when considering these results, mRNA expression may correlate poorly with levels of TR protein. Our results indicate that unpolarized macrophage, M1, and M2 cells expressed TRβ1 protein at the intracellular level,

whereas TRα1 protein was undetectable. In agreement with mRNA data, M2 expressed higher levels of TRβ. At the mRNA and/or protein level, the presence of TRα1 and TRβ1 was reported in rat skeletal mast cells and human bone marrow CD34<sup>+</sup> cells,<sup>58,61</sup> as well as at different stages of mouse dendritic cell maturation.<sup>11,12</sup>

We show the following in bone marrow-derived macrophages: i) only TRβ1 is expressed in differentiated unpolarized macrophages and M1/M2 activated cells, ii) T<sub>3</sub> in differentiated macrophages significantly decreases the expression of TRβ1, and iii) TRβ1 is strongly up-regulated in M2 cells. Collectively, these data suggest a major functional role of TRβ1 in mediating T<sub>3</sub> effects, including the

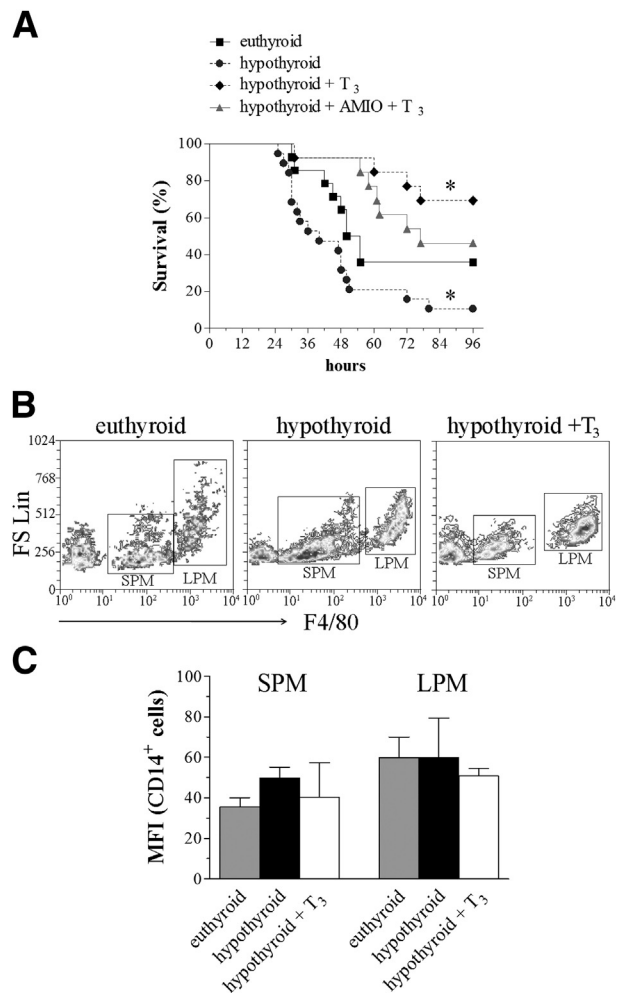


**Figure 10** T<sub>3</sub> and survival in murine endotoxemia induced by i.p. injection with LPS. **A:** Percentage survival (Kaplan-Meier curve, *n* = 13 to 18) of euthyroid and hypothyroid mice. Hypothyroid mice were also injected i.p. with 0.2 μg/g body weight per day T<sub>3</sub> alone or with 20 μg/g body weight per day of AMIO for 5 days before the onset of endotoxemia. \**P* < 0.05 versus euthyroid value. **B** and **C:** Cell surface analysis by flow cytometry of isolated peritoneal cavity cells in euthyroid and hypothyroid mice and in hypothyroid mice injected i.p. for 5 days with 0.2 μg/g body weight per day T<sub>3</sub>. Mice were injected with LPS for 16 hours. **B:** Gating strategy used to identify the macrophage subsets of large cells expressing high levels of F4/80 (LPM) and small cells expressing low levels of F4/80 (SPM). FSLin, forward scatter in linear mode (cell size) (*n* = 3 to 4). **C:** Analysis of CD14 expression (MFI ± SEM) on LPM and SPM F4/80<sup>+</sup> cells (*n* = 3 to 4).

promotion of unpolarized macrophage cells toward the M1 versus M2 signature. This issue, however, deserves further investigations. Of interest, TR $\beta$ 1 was shown to mediate the T<sub>3</sub>-induced maturation and signaling of mouse dendritic cells.<sup>11,12</sup>

### *In Vivo* Results

Given the effects of T<sub>3</sub> on unpolarized macrophage maturation *in vitro*, we investigated the effects of THs in the modulation of macrophage phenotype/recruitment *in vivo*. Although macrophages were historically considered to be derived from the blood monocyte reservoir, numerous studies have since demonstrated that, under steady-state conditions, resident tissue macrophage populations are largely maintained through local proliferation.<sup>86</sup> Inflammatory insults, however, result in the rapid recruitment of blood-borne precursors to the respective tissue macrophage compartment.<sup>86</sup> Our data demonstrate that circulating T<sub>3</sub> increased the content of LPMs, the resident macrophages in the peritoneal cavity,<sup>56</sup> while reducing the content of SPMs, the recruited monocyte-derived cells.<sup>56</sup> The half-life of macrophages in tissues varies from a few days up to several months. Thus, the decreased content of LPM cells in hypothyroid mice may account, at least in part, on the effect of T<sub>3</sub> levels on macrophages that were in the peritoneal cavity at the beginning of the hypothyroid model and were still there when the analysis was done.

Tissue macrophages, and newly recruited monocytes, ensure baseline tissue homeostasis and prevent constant inflammation.<sup>13,22</sup> Classic inflammatory stimuli, such as microbial insult (ie, LPS), frequently occur with concomitant type 2 helper T cell (Th2) cytokine (ie, IL-4) production. It has been recently shown that both resident and recruited (ie, LPM and SPM, respectively, as identified in our model) mouse macrophages can be activated and driven to proliferate by a Th2 environment *in vivo*.<sup>71</sup> It was demonstrated that a Th2 environment was sufficient to drive accumulation of tissue macrophages through self-renewal, indicating that the mechanism of local expansion in type 2 inflammation does not require enhanced bone marrow activity and may deliberately avoid inflammatory cell recruitment and the associated potential for tissue damage.<sup>71</sup> Thus, the proliferation *in situ* has been proposed as an alternative mechanism of inflammation that allows macrophages to accumulate in sufficient numbers to perform critical functions in the absence of potentially damaging cell recruitment.<sup>71</sup> In light of these observations, it is tempting to speculate that T<sub>3</sub> contributes to limit inflammation by promoting the proliferation of macrophages *in situ*, while inhibiting the potentially damaging cell recruitment from monocyte cell pools. Accordingly, we show that circulating T<sub>3</sub> significantly protected mice against inflammation induced by LPS i.p. injection, a model of endotoxemia resembling sepsis.<sup>45,57</sup> This is consistent with previous observations that high circulating levels of THs oppose proinflammatory mechanisms in which monocytes

and macrophages are involved, although discrepancies on TH effects have been also reported.<sup>6</sup> Our findings are in good agreement with published reports on the beneficial role of THs in mice with severe meningococcal sepsis symptoms<sup>20</sup> or in rats during severe sepsis induced by cecal ligation and puncture.<sup>87,88</sup> Relevant data on TH levels as indicators of sepsis severity and predictors of mortality come from human studies. For instance, in patients with septic shock, tissue responses are orientated to decrease production and increase degradation (muscle) or decrease uptake (adipose tissue) of T<sub>3</sub>, as well as to decrease thyroid hormone actions.<sup>89</sup> In addition, T<sub>3</sub> levels were significantly lower in patients with sepsis compared with patients with an inflammatory response without underlying infection,<sup>90</sup> and the levels of THs have been found to be a parameter for evaluating meningococcal septic shock severity.<sup>91,92</sup> A systematic review regarding the association between thyroid hormone abnormalities and the outcome of patients with sepsis or septic shock suggests the existence of an association between lower T<sub>3</sub> or T<sub>4</sub> and worse outcome, although definite conclusions on the described issue cannot be drawn on the basis of the data available.<sup>93</sup> In this respect, because thyroid hormone abnormalities are common in septic patients, future studies should aim to more clearly establish the strength of the previously mentioned association and to determine whether TH supplementation could be beneficial for the outcome of septic patients.

The functional plasticity of macrophages in the course of inflammation and its resolution serve as a means of regulating inflammation in space and time,<sup>94</sup> and sepsis is a case of deregulated inflammation.<sup>95</sup> Although the mechanisms by which T<sub>3</sub> protects mice against LPS-induced endotoxemia are unclear, the use of hypothyroid mice provides evidence that decreased T<sub>3</sub> levels increased SPM frequencies induced by LPS i.p. injection; however, the restoration of T<sub>3</sub> levels decreases SPM and increases LPM frequencies. This suggests that the anti-inflammatory effect of the T<sub>3</sub> system is coupled to the functional modulation of SPM (potentially damaging recruited from bone marrow-derived cells) and LPM (potentially beneficial resident) subsets.<sup>56,71</sup> This is consistent with our *in vitro* results showing a negative role of T<sub>3</sub> in triggering the differentiation of macrophages from bone marrow-derived cells. The fact that peritoneal macrophages expressed TR $\beta$ 1 protein, whereas TR $\alpha$ 1 detection failed, and that the TR $\alpha$ 1/ $\beta$ 1 antagonist, AMIO, inhibited T<sub>3</sub>-induced protection against LPS-induced endotoxemia strongly suggest TR $\beta$ 1 as the major player mediating T<sub>3</sub> effects *in vivo*, in agreement with the *in vitro* results. THs have been recently suggested to control meningococcal septicemia in mice by up-regulating the macrophage production of nitric oxide,<sup>20</sup> a well-established marker of the M1 phenotype.<sup>13,22,28</sup> In this regard, *in vivo* stimulation would classify SPMs and LPMs as M1 cells because both produce large amounts of nitric oxide in response to LPS.<sup>56</sup> Thus, the fact that the M1/M2 framework does not readily accommodate the SPM and LPM subsets should be considered. Our *in vivo* data suggest

that T<sub>3</sub> protection against LPS-induced endotoxemia is caused more by changes in macrophage migration than the differential expression of M1 markers. Accordingly, during the early phase of inflammation, M1 macrophages mediate microbicidal activity, recruitment, and activation of adaptive immune cells and trigger a full-fledged inflammatory response, whereas, during resolution, these cells switch to an anti-inflammatory and tissue remodeling mode.<sup>94</sup>

## Conclusions

The balance of a positive action of T<sub>3</sub> in inflammation versus a potential detrimental one because of the novel link between THs and macrophage maturation we demonstrate opens new perspectives on the interactions between the endocrine and immune systems. The key role of T<sub>3</sub> in inhibiting the differentiation of monocytes into macrophages, while favoring the M1 activation, indicates that this hormone has significant functions in the regulation of immune responses. The increase of resident versus monocyte-recruited macrophages may be an important effector of T<sub>3</sub>-induced protection against the systemic inflammatory response of endotoxemia, which may be developed in therapeutic strategies to counteract pathological conditions disregulating, at least in part, TH homeostasis.

## Acknowledgment

We thank Dr. Silvia Alboni (Università di Modena e Reggio Emilia, Italy) for helping in primer design.

## Supplemental Data

Supplemental material for this article can be found at <http://dx.doi.org/10.1016/j.ajpath.2013.10.006>.

## References

- Butts CL, Sternberg EM: Neuroendocrine factors alter host defense by modulating immune function. *Cell Immunol* 2008, 252:7–15
- Barnard A, Layton D, Hince M, Sakkal S, Bernard C, Chidgey A, Boyd R: Impact of the neuroendocrine system on thymus and bone marrow function. *Neuroimmunomodulation* 2008, 15:7–18
- Rivest S: Interactions between the immune and neuroendocrine systems. *Prog Brain Res* 2010, 181:43–53
- Kelley KW, Weigent DA, Kooijman R: Protein hormones and immunity. *Brain Behav Immun* 2007, 21:384–392
- Carlton ED, Demas GE, French SS: Leptin, a neuroendocrine mediator of immune responses, inflammation, and sickness behaviors. *Horm Behav* 2012, 62:272–279
- De Vito P, Incerpi S, Pedersen JZ, Luly P, Davis FB, Davis PJ: Thyroid hormones as modulators of immune activities at the cellular level. *Thyroid* 2011, 21:879–890
- Cheng SY, Leonard JL, Davis PJ: Molecular aspects of thyroid hormone actions. *Endocr Rev* 2010, 31:139–170
- Yen PM, Ando S, Feng X, Liu Y, Maruvada P, Xia X: Thyroid hormone action at the cellular, genomic and target gene levels. *Mol Cell Endocrinol* 2006, 246:121–127
- Dorshkind K, Horseman ND: The roles of prolactin, growth hormone, insulin-like growth factor-I, and thyroid hormones in lymphocyte development and function: insights from genetic models of hormone and hormone receptor deficiency. *Endocr Rev* 2000, 21:292–312
- Klecha AJ, Genaro AM, Gorelik G, Barreiro Arcos ML, Silberman DM, Schuman M, Garcia SI, Pirola C, Cremaschi GA: Integrative study of hypothalamus-pituitary-thyroid-immune system interaction: thyroid hormone-mediated modulation of lymphocyte activity through the protein kinase C signaling pathway. *J Endocrinol* 2006, 189:45–55
- Mascanfroni I, Montesinos Mdel M, Susperreguy S, Cervi L, Ilarregui JM, Ramseyer VD, Masini-Repiso AM, Targovnik HM, Rabinovich GA, Pellizas CG: Control of dendritic cell maturation and function by triiodothyronine. *FASEB J* 2008, 22:1032–1042
- Mascanfroni ID, Montesinos Mdel M, Alamino VA, Susperreguy S, Nicola JP, Ilarregui JM, Masini-Repiso AM, Rabinovich GA, Pellizas CG: Nuclear factor (NF)-kappaB-dependent thyroid hormone receptor beta1 expression controls dendritic cell function via Akt signaling. *J Biol Chem* 2010, 285:9569–9582
- Murray PJ, Wynn TA: Protective and pathogenic functions of macrophage subsets. *Nat Rev Immunol* 2011, 11:723–737
- Galli SJ, Borregaard N, Wynn TA: Phenotypic and functional plasticity of cells of innate immunity: macrophages, mast cells and neutrophils. *Nat Immunol* 2011, 12:1035–1044
- Rittenhouse PA, Redei E: Thyroxine administration prevents streptococcal cell wall-induced inflammatory responses. *Endocrinology* 1997, 138:1434–1439
- Rosa LF, Safi DA, Curi R: Effect of hypo- and hyperthyroidism on the function and metabolism of macrophages in rats. *Cell Biochem Funct* 1995, 13:141–147
- Forner MA, Barriga C, Ortega E: Exercise-induced stimulation of murine macrophage phagocytosis may be mediated by thyroxine. *J Appl Physiol* 1996, 80:899–903
- El-Shaikh KA, Gabry MS, Othman GA: Recovery of age-dependent immunological deterioration in old mice by thyroxine treatment. *J Anim Physiol Anim Nutr (Berl)* 2006, 90:244–254
- Khansari DN, Murgu AJ, Faith RE: Effects of stress on the immune system. *Immunol Today* 1990, 11:170–175
- Chen Y, Sjolinder M, Wang X, Altenbacher G, Hagner M, Berglund P, Gao Y, Lu T, Jonsson AB, Sjolinder H: Thyroid hormone enhances nitric oxide-mediated bacterial clearance and promotes survival after meningococcal infection. *PLoS One* 2012, 7: e41445
- Ortega E, Forner MA, Garcia JJ, Rodriguez AB, Barriga C: Enhanced chemotaxis of macrophages by strenuous exercise in trained mice: thyroid hormones as possible mediators. *Mol Cell Biochem* 1999, 201:41–47
- Sica A, Mantovani A: Macrophage plasticity and polarization: in vivo veritas. *J Clin Invest* 2012, 122:787–795
- Biswas SK, Mantovani A: Macrophage plasticity and interaction with lymphocyte subsets: cancer as a paradigm. *Nat Immunol* 2010, 11: 889–896
- Martinez FO, Sica A, Mantovani A, Locati M: Macrophage activation and polarization. *Front Biosci* 2008, 13:453–461
- Flamant F, Gauthier K: Thyroid hormone receptors: the challenge of elucidating isotype-specific functions and cell-specific response. *Biochim Biophys Acta* 2013, 1830:3900–3907
- Barish GD, Downes M, Alaynick WA, Yu RT, Ocampo CB, Bookout AL, Mangelsdorf DJ, Evans RM: A nuclear receptor atlas: macrophage activation. *Mol Endocrinol* 2005, 19:2466–2477
- Corna G, Campana L, Pignatti E, Castiglioni A, Tagliafico E, Bosurgi L, Campanella A, Brunelli S, Manfredi AA, Apostoli P, Silvestri L, Camaschella C, Rovere-Querini P: Polarization dictates iron handling by inflammatory and alternatively activated macrophages. *Haematologica* 2010, 95:1814–1822
- Vereyken EJ, Heijnen PD, Baron W, de Vries EH, Dijkstra CD, Teunissen CE: Classically and alternatively activated bone marrow



- derived macrophages differ in cytoskeletal functions and migration towards specific CNS cell types. *J Neuroinflammation* 2011, 8:58
29. Verreck FA, de Boer T, Langenberg DM, van der Zanden L, Ottenhoff TH: Phenotypic and functional profiling of human proinflammatory type-1 and anti-inflammatory type-2 macrophages in response to microbial antigens and IFN-gamma- and CD40L-mediated costimulation. *J Leukoc Biol* 2006, 79:285–293
  30. Davis FB, Tang HY, Shih A, Keating T, Lansing L, Hercbergs A, Fenstermaker RA, Mousa A, Mousa SA, Davis PJ, Lin HY: Acting via a cell surface receptor, thyroid hormone is a growth factor for glioma cells. *Cancer Res* 2006, 66:7270–7275
  31. van den Berg TK, Kraal G: A function for the macrophage F4/80 molecule in tolerance induction. *Trends Immunol* 2005, 26:506–509
  32. Martinez-Pomares L, Platt N, McKnight AJ, DaSilva RP, Gordon S: Macrophage membrane molecules: markers of tissue differentiation and heterogeneity. *Immunobiology* 1996, 195:407–416
  33. Ferenbach D, Hughes J: Macrophages and dendritic cells: what is the difference? *Kidney Int* 2008, 74:5–7
  34. Hume DA: Macrophages as APC and the dendritic cell myth. *J Immunol* 2008, 181:5829–5835
  35. Furness SG, McNagny K: Beyond mere markers: functions for CD34 family of sialomucins in hematopoiesis. *Immunol Res* 2006, 34:13–32
  36. Livak KJ, Schmittgen TD: Analysis of relative gene expression data using real-time quantitative PCR and the 2-DDCT Method. *Methods* 2001, 25:402–408
  37. Cervia D, Martini D, Ristori C, Catalani E, Timperio AM, Bagnoli P, Casini G: Modulation of the neuronal response to ischaemia by somatostatin analogues in wild-type and knock-out mouse retinas. *J Neurochem* 2008, 106:2224–2235
  38. Cervia D, Garcia-Gil M, Simonetti E, Di Giuseppe G, Guella G, Bagnoli P, Dini F: Molecular mechanisms of euplotin C-induced apoptosis: involvement of mitochondrial dysfunction, oxidative stress and proteases. *Apoptosis* 2007, 12:1349–1363
  39. Armani C, Catalani E, Balbarini A, Bagnoli P, Cervia D: Expression, pharmacology, and functional role of somatostatin receptor subtypes 1 and 2 in human macrophages. *J Leukoc Biol* 2007, 81:845–855
  40. Cervia D, Martini D, Garcia-Gil M, Di Giuseppe G, Guella G, Dini F, Bagnoli P: Cytotoxic effects and apoptotic signalling mechanisms of the sesquiterpenoid euplotin C, a secondary metabolite of the marine ciliate *Euplotes crassus*, in tumour cells. *Apoptosis* 2006, 11:829–843
  41. Perrotta C, Bizzozero L, Cazzato D, Morlacchi S, Assi E, Simbari F, Zhang Y, Gulbins E, Bassi MT, Rosa P, Clementi E: Syntaxin 4 is required for acid sphingomyelinase activity and apoptotic function. *J Biol Chem* 2010, 285:40240–40251
  42. Perrotta C, Bizzozero L, Falcone S, Rovere-Querini P, Prinetti A, Schuchman EH, Sonnino S, Manfredi AA, Clementi E: Nitric oxide boosts chemoimmunotherapy via inhibition of acid sphingomyelinase in a mouse model of melanoma. *Cancer Res* 2007, 67:7559–7564
  43. Sodhi A, Tripathi A: Prolactin and growth hormone induce differential cytokine and chemokine profile in murine peritoneal macrophages in vitro: involvement of p-38 MAP kinase, STAT3 and NF-kappaB. *Cytokine* 2008, 41:162–173
  44. Perri SR, Annabi B, Galipeau J: Angiostatin inhibits monocyte/macrophage migration via disruption of actin cytoskeleton. *FASEB J* 2007, 21:3928–3936
  45. Imtiyaz HZ, Williams EP, Hickey MM, Patel SA, Durham AC, Yuan LJ, Hammond R, Gimotty PA, Keith B, Simon MC: Hypoxia-inducible factor 2alpha regulates macrophage function in mouse models of acute and tumor inflammation. *J Clin Invest* 2010, 120:2699–2714
  46. Martinez-Iglesias O, Garcia-Silva S, Regadera J, Aranda A: Hypothyroidism enhances tumor invasiveness and metastasis development. *PLoS One* 2009, 4:e6428
  47. Lima FR, Gervais A, Colin C, Izembart M, Neto VM, Mallat M: Regulation of microglial development: a novel role for thyroid hormone. *J Neurosci* 2001, 21:2028–2038
  48. Amma LL, Campos-Barros A, Wang Z, Vennstrom B, Forrest D: Distinct tissue-specific roles for thyroid hormone receptors beta and alpha1 in regulation of type 1 deiodinase expression. *Mol Endocrinol* 2001, 15:467–475
  49. Dayan CM: Interpretation of thyroid function tests. *Lancet* 2001, 357:619–624
  50. Trajkovic M, Visser TJ, Mittag J, Horn S, Lukas J, Darras VM, Raivich G, Bauer K, Heuer H: Abnormal thyroid hormone metabolism in mice lacking the monocarboxylate transporter 8. *J Clin Invest* 2007, 117:627–635
  51. Rosene ML, Wittmann G, Arrojo e Drigo R, Singru PS, Lechan RM, Bianco AC: Inhibition of the type 2 iodothyronine deiodinase underlies the elevated plasma TSH associated with amiodarone treatment. *Endocrinology* 2010, 151:5961–5970
  52. Brown NS, Smart A, Sharma V, Brinkmeier ML, Greenlee L, Camper SA, Jensen DR, Eckel RH, Krezel W, Chambon P, Haugen BR: Thyroid hormone resistance and increased metabolic rate in the RXR-gamma-deficient mouse. *J Clin Invest* 2000, 106:73–79
  53. Inaba H, Pan D, Shin YH, Martin W, Buchman G, De Groot LJ: Immune response of mice transgenic for human histocompatibility leukocyte antigen-DR to human thyrotropin receptor-extracellular domain. *Thyroid* 2009, 19:1271–1280
  54. Verga Falzacappa C, Mangialardo C, Madaro L, Ranieri D, Lupoi L, Stigliano A, Torrisi MR, Bouche M, Toscano V, Misiti S: Thyroid hormone T3 counteracts STZ induced diabetes in mouse. *PLoS One* 2011, 6:e19839
  55. van Beeren HC, Bakker O, Wiersinga WM: Structure-function relationship of the inhibition of the 3,5,3'-triiodothyronine binding to the alpha1- and beta1-thyroid hormone receptor by amiodarone analogs. *Endocrinology* 1996, 137:2807–2814
  56. Ghosh EE, Cassado AA, Govoni GR, Fukuhara T, Yang Y, Monack DM, Bortoluci KR, Almeida SR, Herzenberg LA: Two physically, functionally, and developmentally distinct peritoneal macrophage subsets. *Proc Natl Acad Sci U S A* 2010, 107:2568–2573
  57. Yang J, Xu J, Chen X, Zhang Y, Jiang X, Guo X, Zhao G: Decrease of plasma platelet-activating factor acetylhydrolase activity in lipopolysaccharide induced mongolian gerbil sepsis model. *PLoS One* 2010, 5:e9190
  58. Grymula K, Paczkowska E, Dziedziczko V, Baskiewicz-Masiuk M, Kawa M, Baumert B, Celewicz Z, Gawrych E, Machalinski B: The influence of 3,3',5-triiodo-L-thyronine on human haematopoiesis. *Cell Prolif* 2007, 40:302–315
  59. Abel ED, Boers ME, Pazos-Moura C, Moura E, Kaulbach H, Zakaria M, Lowell B, Radovick S, Liberman MC, Wondisford F: Divergent roles for thyroid hormone receptor beta isoforms in the endocrine axis and auditory system. *J Clin Invest* 1999, 104:291–300
  60. Schwartz HL, Lazar MA, Oppenheimer JH: Widespread distribution of immunoreactive thyroid hormone beta 2 receptor (TR beta 2) in the nuclei of extrapituitary rat tissues. *J Biol Chem* 1994, 269:24777–24782
  61. Siebler T, Robson H, Bromley M, Stevens DA, Shalet SM, Williams GR: Thyroid status affects number and localization of thyroid hormone receptor expressing mast cells in bone marrow. *Bone* 2002, 30:259–266
  62. Borngraeber S, Budny MJ, Chiellini G, Cunha-Lima ST, Togashi M, Webb P, Baxter JD, Scanlan TS, Fletterick RJ: Ligand selectivity by seeking hydrophobicity in thyroid hormone receptor. *Proc Natl Acad Sci U S A* 2003, 100:15358–15363
  63. Davis PJ, Leonard JL, Davis FB: Mechanisms of nongenomic actions of thyroid hormone. *Front Neuroendocrinol* 2008, 29:211–218
  64. Lin HY, Sun M, Tang HY, Lin C, Luidens MK, Mousa SA, Incerpi S, Drusano GL, Davis FB, Davis PJ: L-Thyroxine vs. 3,5,3'-triiodo-L-thyronine and cell proliferation: activation of mitogen-activated

- protein kinase and phosphatidylinositol 3-kinase. *Am J Physiol Cell Physiol* 2009, 296:C980–C991
65. Westerholz S, de Lima AD, Voigt T: Regulation of early spontaneous network activity and GABAergic neurons development by thyroid hormone. *Neuroscience* 2010, 168:573–589
  66. Schapira M, Raaka BM, Das S, Fan L, Totrov M, Zhou Z, Wilson SR, Abagyan R, Samuels HH: Discovery of diverse thyroid hormone receptor antagonists by high-throughput docking. *Proc Natl Acad Sci U S A* 2003, 100:7354–7359
  67. Lee JY, Takahashi N, Yasubuchi M, Kim YI, Hashizaki H, Kim MJ, Sakamoto T, Goto T, Kawada T: Triiodothyronine induces UCP-1 expression and mitochondrial biogenesis in human adipocytes. *Am J Physiol Cell Physiol* 2012, 302:C463–C472
  68. Briken V, Mosser DM: Editorial: switching on arginase in M2 macrophages. *J Leukoc Biol* 2011, 90:839–841
  69. Sica A, Bronte V: Altered macrophage differentiation and immune dysfunction in tumor development. *J Clin Invest* 2007, 117:1155–1166
  70. Ohashi K, Parker JL, Ouchi N, Higuchi A, Vita JA, Gokce N, Pedersen AA, Kalthoff C, Tullin S, Sams A, Summer R, Walsh K: Adiponectin promotes macrophage polarization toward an anti-inflammatory phenotype. *J Biol Chem* 2010, 285:6153–6160
  71. Jenkins SJ, Ruckerl D, Cook PC, Jones LH, Finkelman FD, van Rooijen N, MacDonald AS, Allen JE: Local macrophage proliferation, rather than recruitment from the blood, is a signature of TH2 inflammation. *Science* 2011, 332:1284–1288
  72. Belikoff BG, Hatfield S, Georgiev P, Ohta A, Lukashev D, Buras JA, Remick DG, Sitkovsky M: A2B adenosine receptor blockade enhances macrophage-mediated bacterial phagocytosis and improves polymicrobial sepsis survival in mice. *J Immunol* 2011, 186:2444–2453
  73. Rickard AJ, Young MJ: Corticosteroid receptors, macrophages and cardiovascular disease. *J Mol Endocrinol* 2009, 42:449–459
  74. Lu C, Kumar PA, Fan Y, Sperling MA, Menon RK: A novel effect of growth hormone on macrophage modulates macrophage-dependent adipocyte differentiation. *Endocrinology* 2010, 151:2189–2199
  75. Leonard JL, Larsen PR: Thyroid hormone metabolism in primary cultures of fetal rat brain cells. *Brain Res* 1985, 327:1–13
  76. Garcia-Silva S, Aranda A: The thyroid hormone receptor is a suppressor of ras-mediated transcription, proliferation, and transformation. *Mol Cell Biol* 2004, 24:7514–7523
  77. Forini F, Paolicchi A, Pizzorusso T, Ratto GM, Saviozzi M, Vanini V, Iervasi G: 3,5,3'-Triiodothyronine deprivation affects phenotype and intracellular [Ca<sup>2+</sup>]<sub>i</sub> of human cardiomyocytes in culture. *Cardiovasc Res* 2001, 51:322–330
  78. Fragner P, Ladram A, Aratan de Leon S: Triiodothyronine down-regulates thyrotropin-releasing hormone (TRH) synthesis and decreases pTRH-(160-169) and insulin releases from fetal rat islets in culture. *Endocrinology* 1999, 140:4113–4119
  79. Morte B, Diez D, Auso E, Belinchon MM, Gil-Ibanez P, Grijota-Martinez C, Navarro D, de Escobar GM, Berbel P, Bernal J: Thyroid hormone regulation of gene expression in the developing rat fetal cerebral cortex: prominent role of the Ca<sup>2+</sup>/calmodulin-dependent protein kinase IV pathway. *Endocrinology* 2010, 151:810–820
  80. Yehuda-Shnaidman E, Kalderon B, Azazmeh N, Bar-Tana J: Gating of the mitochondrial permeability transition pore by thyroid hormone. *FASEB J* 2010, 24:93–104
  81. Gosteli-Peter MA, Harder BA, Eppenberger HM, Zapf J, Schaub MC: Triiodothyronine induces over-expression of alpha-smooth muscle actin, restricts myofibrillar expansion and is permissive for the action of basic fibroblast growth factor and insulin-like growth factor I in adult rat cardiomyocytes. *J Clin Invest* 1996, 98:1737–1744
  82. Sanchez-Pacheco A, Aranda A: Binding of the thyroid hormone receptor to a negative element in the basal growth hormone promoter is associated with histone acetylation. *J Biol Chem* 2003, 278:39383–39391
  83. Nevado J, Tenbaum SP, Aranda A: hSrb7, an essential human mediator component, acts as a coactivator for the thyroid hormone receptor. *Mol Cell Endocrinol* 2004, 222:41–51
  84. Yehuda-Shnaidman E, Kalderon B, Bar-Tana J: Modulation of mitochondrial transition pore components by thyroid hormone. *Endocrinology* 2005, 146:2462–2472
  85. Geissmann F, Manz MG, Jung S, Sieweke MH, Merad M, Ley K: Development of monocytes, macrophages, and dendritic cells. *Science* 2010, 327:656–661
  86. Yona S, Jung S: Monocytes: subsets, origins, fates and functions. *Curr Opin Hematol* 2010, 17:53–59
  87. Al-Abed Y, Metz CN, Cheng KF, Aljabari B, VanPatten S, Blau S, Lee H, Ochani M, Pavlov VA, Coleman T, Meurice N, Tracey KJ, Miller EJ: Thyroxine is a potential endogenous antagonist of macrophage migration inhibitory factor (MIF) activity. *Proc Natl Acad Sci U S A* 2011, 108:8224–8227
  88. Inan M, Koyuncu A, Aydin C, Turan M, Gokgoz S, Sen M: Thyroid hormone supplementation in sepsis: an experimental study. *Surg Today* 2003, 33:24–29
  89. Rodriguez-Perez A, Palos-Paz F, Kaptein E, Visser TJ, Dominguez-Gerpe L, Alvarez-Escudero J, Lado-Abeal J: Identification of molecular mechanisms related to nonthyroidal illness syndrome in skeletal muscle and adipose tissue from patients with septic shock. *Clin Endocrinol (Oxf)* 2008, 68:821–827
  90. Koenig KF, Potlukova E, Mueller B, Christ-Crain M, Trendelenburg M: MBL serum levels in patients with sepsis correlate with thyroid function but not with outcome. *Clin Immunol* 2012, 144:80–82
  91. den Brinker M, Dumas B, Visser TJ, Hop WC, Hazelzet JA, Festen DA, Hokken-Koelega AC, Joosten KF: Thyroid function and outcome in children who survived meningococcal septic shock. *Intensive Care Med* 2005, 31:970–976
  92. den Brinker M, Joosten KF, Visser TJ, Hop WC, de Rijke YB, Hazelzet JA, Boonstra VH, Hokken-Koelega AC: Euthyroid sick syndrome in meningococcal sepsis: the impact of peripheral thyroid hormone metabolism and binding proteins. *J Clin Endocrinol Metab* 2005, 90:5613–5620
  93. Angelousi AG, Karageorgopoulos DE, Kapaskelis AM, Falagas ME: Association between thyroid function tests at baseline and the outcome of patients with sepsis or septic shock: a systematic review. *Eur J Endocrinol* 2011, 164:147–155
  94. Biswas SK, Chittezhath M, Shalova IN, Lim JY: Macrophage polarization and plasticity in health and disease. *Immunol Res* 2012, 53:11–24
  95. Hotchkiss RS, Coopersmith CM, McDunn JE, Ferguson TA: The sepsis seesaw: tilting toward immunosuppression. *Nat Med* 2009, 15:496–497